2

Jackson, C. A.-L., 2007, The geometry, distribution, and development of clastic injections in slope systems: Seismic examples from the Upper Cretaceous Kyrre Formation, Måløy slope, Norwegian margin, *in* A. Hurst and J. Cartwright, eds., Sand injectites: Implications for hydrocarbon exploration and production: AAPG Memoir 87, p. 37–48.

The Geometry, Distribution, and Development of Clastic Injections in Slope Systems: Seismic Examples from the Upper Cretaceous Kyrre Formation, Måløy Slope, Norwegian Margin

Christopher A.-L. Jackson[1]

Norsk Hydro Research Center, Bergen, Norway

ABSTRACT

An integrated three-dimensional seismic, well, and core study indicates the development of a series of slope channel and fan-depositional systems in the Upper Cretaceous interval of the Måløy slope, Norwegian margin. Because of their sand content and occurrence in a mud-dominated succession, the slope-depositional systems manifest as high-amplitude reflection packages on seismic reflection data. The Upper Cretaceous depositional systems are flanked and overlain by two types of amplitude anomalies that display unusual geometries in cross section and plan view. The first type of anomaly is bedding discordant and crosscuts overlying reflections, dips 10–20°, is as much as 100 ms high, and is typically developed at the margins of the slope systems. The second type of amplitude anomaly is bedding concordant, as much as 400 m (1312 ft) long in cross section, and is developed either halfway up or at the upper tips of the bedding discordant anomalies. In three dimensions, the steeply dipping anomalies developed at the margins of the slope-depositional systems form winglike structures that are elongate along the lengths of the slope-depositional systems. Based on their close spatial relationship to the Upper Cretaceous slope-depositional systems and inferred sand content, the bedding-discordant and bedding-concordant amplitude anomalies are interpreted as clastic dikes and sills, respectively, sourced from the Upper Cretaceous slope systems. Although the mechanism that caused initial overpressuring of the sand bodies is unclear, it is speculated that a combination of the migration of basinal fluids into the sealed depositional sand bodies and rapid burial of the sand bodies in low-permeability mudstones may have contributed. The development of the largest clastic dikes at the margins of the depositional systems suggests that differential compaction and forced

[1]*Present address*: Department of Earth Sciences and Engineering, Imperial College, London, United Kingdom.

DOI:10.1306/1209848M873254

folding adjacent to the buried depositional systems triggered remobilization and injection and the subsequent geometry and distribution of clastic injection features. The postdepositional remobilization and injection of clastic slope systems as exemplified in this study have important implications for hydrocarbon exploration and production in slope systems because this process has caused marked changes in primary reservoir geometry and has resulted in the development of clastic intrusions that are large enough to represent stand-alone exploration targets.

INTRODUCTION

An increasing number of outcrop and subsurface studies recognize the importance of clastic remobilization and injection in the geometric and lithological modification of slope sand bodies. Clastic remobilization and injection of slope sand systems have been identified at a variety of scales, from centimeter-scale dikes and sills (e.g., Hiscott, 1979; Archer, 1984; St. J. Newman et al., 1993; Dixon et al., 1995; Bergslien, 2002; Duranti et al., 2002; Hillier and Cosgrove, 2002; Purvis et al., 2002), to seismic-scale complexes featuring dikes as much as 40 m (131 ft) thick and more than 200 m (660 ft) high (e.g., Lonergan and Cartwright, 1999; Cosgrove and Hillier, 2000; Bergslien, 2002; Molyneux et al., 2002; Huuse et al., 2003, 2004; Huuse and Mickelson, 2004; Shoulders and Cartwright, 2004). At all these scales, remobilization and injection have been demonstrated to have major implications for the exploration and development of deep-water systems (see review in Lonergan et al., 2000). For example, several studies have indicated that remobilization and injection can influence reservoir architecture and connectivity, reservoir volumetrics, and pore-scale reservoir properties (Jenssen et al., 1993; Timbrell, 1993; Lonergan and Cartwright, 1999; Duranti et al., 2002). Clastic intrusions must, therefore, be accounted for in three-dimensional (3-D) reservoir modeling (Guargena et al., 2002; Purvis et al., 2002). It is desirable to know to what degree a reservoir sand body has been affected by postdepositional remobilization and injection, and how this modification may affect future production and production planning. Clastic intrusions are commonly at or below the limit of seismic resolution and, accordingly, can be difficult to identify and map in 3-D. Because of this, published examples of the geometry of seismic-scale clastic intrusion complexes have dealt primarily with their two-dimensional geometry (e.g., Lonergan and Cartwright, 1999; MacLeod et al., 1999; Cosgrove and Hillier, 2000; Shoulders and Cartwright, 2004). Those studies that have documented the 3-D seismic expression of clastic injection complexes have been stratigraphically and geographically restricted to Paleocene and Eocene slope and basin-floor systems of the United Kingdom central North Sea (Molyneux et al., 2002; Huuse et al., 2003, 2004; Huuse and Mickelson, 2004). The need for additional seismic studies of clastic intrusion complexes is, therefore, twofold: first, to accurately document the scale, 3-D geometry, and spatial distribution of clastic intrusion complexes; and second, to test existing conceptual models for the development of clastic injection complexes and investigate potential local controls on their development.

The aim of this chapter is to describe the seismic expression of some interpreted clastic injection complexes developed in association with Upper Cretaceous slope systems on the Måløy slope, Norwegian margin (Figure 1), and to discuss the controls on their development. This study is unique because it is the first documented example of seismic-scale, slope system-related, clastic injection complexes in the Upper Cretaceous of the northern North Sea. Furthermore, in contrast to previous seismic studies, the interpreted clastic intrusion complexes are spectacularly imaged on high-quality 3-D seismic data, thereby allowing individual intrusion-related bodies to be mapped in 3-D using a combination of amplitude mapping and volume opacity techniques. Using these mapping methods, both the primary (i.e., depositional) and secondary (i.e., injected) sand bodies can be mapped in 3-D, and their geometry, scale, and distribution can be documented. Based on the tectonic and stratigraphic setting of the Måløy slope during the Late Cretaceous, the factors controlling remobilization and injection are discussed. The chapter concludes with a brief discussion on the implications of clastic intrusion complex development in deep-water depositional systems for hydrocarbon exploration and production.

GEOLOGICAL SETTING

The study area is located on the Måløy slope, one of several structural terraces located along the eastern margin of the Late Jurassic North Sea extensional basin (Figures 1, 2b). The Måløy slope is bounded to the east by the large displacement (5 km; 3 mi) Øygården fault zone and to the west by a major normal fault bounding the eastern margin of the Sogn graben (Figures 1, 2b). Structural mapping at top Brent level (i.e., top prerift with respect to the Upper Jurassic rift event) and thickness variations in the Upper Jurassic synrift strata

indicate that during the main Late Jurassic to Early Cretaceous extensional episode, the Måløy slope was compartmentalized into a series of rotated half grabens bounded by a series of north–south- to north-northwest–south-southeast-striking normal faults (Figure 2b) (Gabrielsen et al., 2001; Fraser et al., 2003). In the Early Cretaceous, the synrift to postrift transition saw a marked change in the geometry of the North Sea Basin. In the study area, this was characterized by a reduction in the rate of normal faulting, an overall decrease in the basin subsidence rate, and the migration of the locus of subsidence into the axis of the north Viking Graben and its northern extension, the Sogn graben. Simultaneously, continental Norway experienced a period of uplift speculated to be linked to the opening of the North Atlantic (Martinsen et al., 1999; Bugge et al., 2001; Gabrielsen et al., 2001). The change in subsidence and uplift patterns, combined with ongoing sedimentation, resulted in infilling and smoothing of the Upper Jurassic rift-related fault-block topography, and the transformation of the Måløy slope into a west-facing, passive margin for much of the Cretaceous and Tertiary (Figures 1–3).

Wire-line–log, core, and biostratigraphic data indicate that the postrift period was dominated by deposition of hemipelagic mudstones and thin carbonates in a slope to base-of-slope setting in bathyal (200–500-m; 660–1640-ft) water depths (Figure 2a) (Bugge et al., 2001; Gabrielsen et al., 2001). Distributed on the mud-dominated slope system are several sandy submarine channels and submarine fans of the Coniacian to early Campanian Kyrre Formation, which are interpreted to have been sourced from the Norwegian hinterland to the west (Bugge et al., 2001; Martinsen et al., 2005) (Figures 2a, 3). Structurally, the Late Cretaceous is interpreted to have been a period of tectonic quiescence. It is speculated, however, that the Øygården fault zone was active at this time, and that the Upper Jurassic Gjøa fault zone was experiencing minor reactivation as indicated by minor offset of Upper Cretaceous strata (Figures 1, 2b). Additional structures observed within the interval of interest include a polygonal fault system (Cartwright, 1994, 1996) and a series of low-relief monoclines (Figure 3). The polygonal fault system is developed within the strata of Lower Cretaceous to upper Tertiary age and is interpreted to have formed in response to dewatering and 3-D contraction of these units during burial and compaction (e.g., Cartwright, 1994; Cartwright and Lonergan, 1996; Dewhurst et al., 1999). The low-relief monoclines are observed throughout much of the Cretaceous section and are interpreted to have formed because of differential compaction of the Cretaceous section over the buried fault-block topography associated with the Late Jurassic Gjøa fault zone (Figure 2b). It is unclear what influence these monoclines had on sedimentation patterns during the Late Cretaceous, but thinning of the Upper Cretaceous strata across the monoclines suggests that they may have formed subtle Late Cretaceous sea-floor highs (Figures 2b, 3) (Martinsen et al., 2005).

DATA SET

The seismic data set consists of two overlapping 3-D seismic surveys that partially cover North Sea exploration blocks 35/6, 35/9, 36/4, and 36/7 (Figure 1). In total, the area of seismic data used in this study is 3000 km^2 (1158 mi^2), with an inline and crossline spacing of 12.5 m (41 ft). None of the surveys are depth converted; thus, all depth measurements are given in two-way traveltime (ms TWTT). The vertical resolution of seismic reflections is a function of the frequency content of the seismic data and the acoustic velocity and present-day burial depth of the studied interval and is estimated to be approximately 30 m (98 ft). Data quality in both surveys is generally good to excellent at the depth interval of study, deteriorating slightly in the westernmost parts of blocks 35/9 and 35/6 because of the presence of gas chimneys that emanate from the underlying Upper Jurassic basins. Both the surveys are zero-phase processed and normal polarity, whereby a positive peak event (black reflection on seismic sections) represents an increase in acoustic impedance with depth, and a negative trough event (red reflection on seismic sections) represents a decrease in acoustic impedance with depth.

The studied interval is penetrated by three exploration wells; 35/9-3, 35/9-3 T2 (sidetrack of 35/9-3), and 36/7-3. All three wells penetrated the distal edge of one of the studied Upper Cretaceous slope systems and have a full suite of wire-line–log data in addition to detailed in-house, biostratigraphic zonations. In addition, both the 35/9-3 and 35/9-3 T2 have excellent core coverage through the studied interest, thereby allowing the observed seismic response to be calibrated to lithology and depositional facies (Figure 4).

LATE CRETACEOUS DEPOSITIONAL SYSTEMS

Three-dimensional seismic data from the Måløy slope indicate the development of a series of amplitude anomalies in the Upper Cretaceous section, which, based on their plan view and cross sectional geometry and ties to wire-line and core data, are interpreted as the seismic expression of a series of slope-depositional systems.

Because of their high-amplitude expression on seismic data, the geometry and distribution of the Late Cretaceous depositional systems are best illustrated on a seismic reflection strength attribute map extracted

285 ms above the base Blødaks seismic horizon (Figure 5a). The map displays three distinct channel-shaped and two fan-shaped amplitude anomalies located in the western and central parts of the study area (channels A, B, and C, and fans A and B; Figure 5a). The largest identified feature is an 18-km (11-mi)-radius, symmetrical fan-shaped amplitude anomaly located in the eastern part of the study area (Figure 5a). East–west-oriented seismic sections across the anomaly indicate that it is composed of a package of high-amplitude parallel reflections as much as 120 ms thick. These reflections thin and onlap onto older units landward toward the east and also thin basinward to the west in association with a marked decrease in seismic amplitude (Figure 2b). North–south-oriented seismic sections indicate that the package of high-amplitude reflections has a mounded, convex-upward cross sectional geometry, with thinning toward the north and south associated with a marked decrease in seismic amplitude (Figure 6a).

Wells 35/9-3, 35/9-3 T2, and 36/7-3 penetrate the distal edge of the large fan-shaped amplitude anomaly (Figure 5b). 35/9-3 T2 has excellent wire-line and core data through the lower part of the Kyrre Formation and indicates that within this interval, four sand-rich units can be observed: a lower, middle to late Turonian–aged unit 16 m (52 ft) thick, and three, Coniacian–aged units between 6 and 12 m (19 and 39 ft) thick (Figure 7). Core through the two uppermost sand units indicates that the sandstones are fine to medium grained and massive to parallel laminated and contain dish structures in their upper parts (Figure 4). Based on these characteristics, the sandstones are interpreted as high-density turbidites deposited in a channelized submarine-fan environment (Martinsen et al., 2005). To allow the observed seismic response to be confidently correlated to lithology and depositional facies interpreted from well and core data, a synthetic seismogram was generated for well 35/9-3 T2 (Figure 7). Log data indicate that the top of the sand-bearing unit is defined by a marked decrease in acoustic impedance (probably related to the gas in the sands); thus, the three Coniacian sand units, which are too thin to be resolved individually, together are represented by a high-amplitude trough (red) event herein termed the ''near-top Kyrre sand event'' (Figure 7). The base of a 16-m (52-ft)-thick, middle to late Turonian–aged unit that developed toward the base of the sand-bearing interval corresponds to a marked increase in acoustic impedance that is represented seismically as a moderate amplitude peak (black) event (Figure 7). By tying the seismic data to the well data in this manner, it is apparent that the fan-shaped amplitude anomaly corresponds to the only substantial sand-bearing interval in the entire Late Cretaceous section. Well 36/7-3, located 8 km (5 mi) southeast of wells 35/9-3 T2, also penetrates the distal margin of the fan-shaped amplitude anomaly (Figure 5b). Synthetic seismograms (not shown) were also constructed for this well and yielded a similar result as that for the 35/9-3 T2 well, with 20 m (66 ft) of massive turbidite sands (interpreted from wire-line–log data) corresponding to the interval of high-amplitude reflections associated with the fan-shaped amplitude anomaly. It is noted that all other wells in blocks 35 and 36, which are located in regions of low to moderate amplitude, chaotic to parallel-bedded seismic facies, did not encounter any sand at this stratigraphic level. Thus, based on its distinctive fan-shaped plan-view geometry, mounded cross sectional geometry, and onlapping relationship with the underlying slope, in addition to tying with turbiditic submarine-fan facies, the fan-shaped amplitude anomaly is interpreted as a submarine slope fan (Figure 5b) (Bugge et al., 2001; Martinsen et al., 2005).

Three channel-shaped seismic anomalies are identified immediately basinward of, and at a slightly lower stratigraphic level than, the submarine slope fan described above. In plan view, the amplitude anomalies are straight to slightly sinuous, 1.2–3 km (0.7–1.8 mi) wide, and trend east–west to east-northeast–west-northwest (Figures 2b; 5a, b). On north-northeast–south-southwest-oriented seismic sections, it is seen that amplitude anomalies are composed of low- to high-amplitude reflection packages as much as 90 ms thick, which have slightly irregular bases and mounded upper surfaces. Internally, they are composed of either flat-lying, high-amplitude, or low-amplitude, chaotic reflection packages (Figure 6b–d). In detail, it is seen that horizons overlying the channel-shaped anomalies, in particular channel units A and B, are quite rugose because of a combination of polygonal faulting (Figure 3) and the occurrence of chaotic and steeply dipping, moderate-amplitude reflectors (Figure 6b, c). Steeply dipping, moderate- to high-amplitude reflections are also observed at the margins of the channel-shaped amplitude anomalies (Figure 6b–d), a detailed description of which will be given in the following section.

Channel C terminates downdip to the west in a fan-shaped amplitude anomaly up to 5.5 km (3.4 mi) wide and 5.5 km (3.4 mi) long (Figure 5a). Seismic sections across the anomaly indicate that it has a slightly erosive base and a flat to slightly undulose upper surface (Figure 6e). Internally, because of the density of polygonal faults deforming the fan, it is commonly difficult to distinguish between primary (i.e., depositional) reflection geometries and those caused by polygonal faulting. Where faulting is less pervasive, it is seen that the fan is composed of a 70–90-ms-thick package of high-amplitude reflections that are either sheetlike and parallel or slightly channelized (Figure 6e).

None of the wells in the study area directly penetrate the channel-shaped amplitude anomalies or the fan-shaped amplitude anomaly developed at the end of channel C; thus, it is therefore difficult to unequivocally demonstrate that their high-amplitude seismic

expression is caused by sand presence (Figure 5a). The channel- and fan-shaped amplitude anomalies are, however, very similar in terms of seismic expression to the sand-bearing slope fan. In particular, the tops of the channel- and fan-shaped anomalies are, in each case, defined by a high-amplitude trough (red) event that is similar to that observed at the top of the sand-bearing interval in the 35/9-3 T2 (Figure 7). Based on the close temporal and spatial relationship to the interpreted sandy submarine slope fan described above, the similar high-amplitude trough (red) event that characterizes the top of the high-amplitude packages, it is inferred that the channel-shaped anomalies are sand rich. Based on their marked channelized plan-view geometries, their slightly erosive bases, their temporal and spatial relationship to the submarine slope fan, and by inference that the anomalies are high amplitude because of the presence of sand, these amplitude anomalies are interpreted as submarine channels (Figure 5b). Pronounced mounding of strata across the amplitude anomalies is interpreted to be the result of differential compaction of the mud-dominated strata adjacent to the channels (cf. Jenssen et al., 1993). Based on its fan-shaped plan-view geometry, its relationship to submarine channel C, and the internal sheet- to channel-like reflectors, the fan-shaped anomaly that developed at the termination of channel C is interpreted as a sheeted to channelized submarine fan (Figure 5b).

The Upper Cretaceous submarine-channel and submarine-fan depositional systems of the Måløy slope display erosive bases and parallel-bedded and/or chaotic, low- to high-amplitude reflectors. Such geometries are commonly observed in association with sandy slope systems (e.g., Mayall and Stewart, 2000; Prather et al., 2000) (Figure 6a–e). However, the small, steeply dipping reflectors developed above the channels, and the steeply dipping and flat-lying high-amplitude reflectors observed at the channel and fan margins (and locally above the channel axes) are not typical geometries observed in slope systems (Figure 6b–e). In the following section, the geometry, scale, distribution, and origin of amplitude anomalies developed adjacent to the Late Cretaceous depositional systems are described.

SLOPE SYSTEM-RELATED AMPLITUDE ANOMALIES

Seismic sections oriented perpendicular to the Late Cretaceous deep-water depositional systems indicate the development of high-amplitude seismic anomalies at their margins (Figure 6b–e). The anomalies that developed at the margins of the submarine channels typically consist of trough-peak reflection couplets that dip 10–20°, and crosscut as much as 100 ms of the overlying stratigraphy before either dimming or shallowing in dip to become concordant with the flat-lying surrounding strata. Although it is difficult to demonstrate that the amplitude anomalies terminate at one particular seismic horizon, it is apparent that they tend to shallow out approximately 75 ms above the interpreted channel base, and none of them extend upward of a moderate-amplitude peak (black) seismic event 50 ms below the near-top Kyrre sand seismic horizon (Figure 6b–e). In addition to flattening out upward, the amplitude anomalies developed adjacent to channel A may also consist of flat-lying portions as much as 400 m (1312 ft) long, which are typically developed halfway up the steeply dipping, channel-margin anomaly and give the anomalies a distinctive dog-leg geometry in cross section. The flat-lying part of these distinct dog-leg anomalies always occur at the same stratigraphic level, approximately 75 ms above the interpreted channel base (Figure 6b).

Because of the quality of the 3-D seismic data set, a combination of traditional line-based mapping and autotracking allows the amplitude anomalies developed at the margins of the depositional systems to be mapped and visualized in 3-D. Mapping indicates that the amplitude anomalies form winglike structures (herein termed ''wings'') that flank the main channel units. At the margins of channels B and C, the wings are planar and more or less continuous along the entire 15-km (9-mi)-long mapped lengths of the channels (Figure 5a). Wing structures flanking channel A show a wider range of geometries and spatial organization. For example, adjacent to channel A, they attain a maximum length of 5 km (3.1 mi) but form an en echelon arrangement of individual wing segments that form a compound wing that flanks the entire length of the channel (Figures 5a, 8). Furthermore, individual segments in the compound wing are either planar, like those developed adjacent to channels B (Figure 9) and C (Figure 10), or strongly arcuate, as developed adjacent to channel A in Figure 5a. A high-amplitude wing is also developed along the southern margin of the small submarine fan associated with channel C. Although similar in height, this feature contrasts with those developed adjacent to the submarine channels because it is laterally less continuous, being only 1 km (0.6 mi) long (Figure 11).

Although amplitude anomalies developed at the margins and above the axes of the depositional systems appear to be dominated by straight to arcuate, planar forms, detailed 3-D mapping indicates marked variability in the geometry of the wings, both between and within individual depositional systems. For example, anomalies flanking channels B and C are typically planar and extend along the entire strike lengths of the channels without any significant variation in dip (Figures 6c, d; 10, 11). In contrast, the geometries of individual anomalies developed adjacent to channel A

are significantly more complex, and marked along-strike variability in geometry is observed. For example, parts of the amplitude anomalies flanking the channel display the simple wing form that is observed adjacent to channels B and C. Locally, however, flat-lying, plateaulike areas are developed along the wings, which, as seismic sections demonstrate, correspond to the flat-lying parts of the dog-leg-type anomalies described previously (Figures 6b, 8). The flat-lying parts of the anomalies are circular to ovate and as much as 1.6×10^5 km^2 (6.1×10^4 mi^2) in area.

Amplitude anomalies that developed at the margins of the depositional systems may also display complex branching forms when traced along strike. This is well illustrated by anomaly A developed along the northern margin of channel unit A (marked A in Figure 8), which has a simple, wing geometry downdip to the west. Updip toward the southeast, an amplitude anomaly consisting of trough-peak reflection pair splays of the channel-margin wing, cutting 50 ms upstratigraphic section toward the axis of the channel and terminating 45 ms below the near-top Kyrre sand seismic horizon (Figure 8). Similar branching forms are also observed locally along the other submarine channels.

Although most commonly observed at the margins of the depositional systems, amplitude anomalies are also observed above the axes of some of the channel units. Mapping and visualization of amplitude anomalies above channel units A and B indicate that they form wing structures that are oriented subparallel to the channel axes and show variable (i.e., north-northeast and south-southwest) dip directions (Figure 8). Although the wings have similar dips (i.e., 10–20°), they are typically much smaller (i.e., 20–50 ms high) and less laterally continuous than those developed at the channel margins. Locally, however, above channels A and B, wings comparable in size to those developed at the channel margins are observed (Figures 6b, d; 8). Steeply dipping channel axes amplitude anomalies may also be spatially related to flat-lying amplitude anomalies that appear to be isolated from the main channel unit below (Figure 6b). These are similar in geometry but smaller in scale to the flat-lying anomalies developed at the channel margins.

ORIGIN OF SLOPE SYSTEM-RELATED AMPLITUDE ANOMALIES

The bedding-discordant and bedding-concordant amplitude anomalies are not reflector geometries commonly associated with sand-bearing slope channel and fan systems (Figures 6a–e; 8, 12). An interpretation of the origin of the slope channel- and fan-related amplitude anomalies must consider the following observations:

- the highly discordant nature of winglike amplitude anomalies with respect to surrounding mudstone-dominated units and their spatial relationship to bedding-concordant amplitude anomalies
- the development of the amplitude anomalies adjacent to the Upper Cretaceous slope-depositional systems
- the physical connection between the amplitude anomalies and the Upper Cretaceous depositional systems
- the high-amplitude expression of the anomalies defined by a upper trough (red) event and a lower peak (black) event

Based on their apparent physical connection to the sand-bearing, Upper Cretaceous depositional systems, the bedding-concordant and bedding-discordant amplitude anomalies may be suggested as the seismic expression of sand-bearing units. Second, both bedding-concordant and bedding-discordant amplitude anomalies are defined by an upper trough (red) event. This seismic response is similar to that which characterizes the top of the sand-bearing slope fan (Figure 7); thus, it is inferred that the decrease in acoustic impedance reflected by this trough (red) event is caused by the presence of sand in the amplitude anomalies. Furthermore, based on the observation that the steeply dipping, channel- and fan-related amplitude anomalies crosscut the surrounding mudstone-dominated units, these apparently sand-bearing features are interpreted to postdate the deposition of these encasing units.

Based on the interpretation of the channel- and fan-related amplitude anomalies as sand bearing, their relationship to sand-bearing slope systems, their complex cross sectional geometries, their relatively late formation with respect to the surrounding sedimentary units, and by analogy to similar features identified in the Eocene and Paleocene strata of the United Kingdom central North Sea, the bedding-discordant and bedding-concordant amplitude anomalies are interpreted as the seismic expression of clastic dikes and clastic sills, respectively, sourced from the Upper Cretaceous depositional sand bodies. Clastic dikes and sills form in response to postdepositional remobilization and injection of sands, and it is generally accepted that there are two main prerequisites for the formation of clastic intrusions. First, the source sand body must be uncemented, such that the sand can be mobilized. Second, the source sand body must be sealed so that an overpressure can be generated within the sand body, and a steep hydraulic gradient is developed at the interface between sand body and the overlying top seal units, thereby allowing the mobilization of sand grains

during top seal failure. Studies of Eocene and Paleocene slope and basin-floor depositional systems indicate that these conditions are most commonly met where sand-rich, turbidite-fed, slope channels, fans, and isolated mounds are deposited on mud-dominated submarine slopes and subsequently encased in low-permeability mudstones. Wire-line and core data from the Kyrre Formation indicate that the slope sand bodies were deposited on a mud-dominated submarine slope and, subsequently encased in low-permeability mudstones, thus had the potential to become overpressured, remobilized, and injected. Once overpressure is developed in sealed sand bodies, a mechanism is required to trigger remobilization of the source sand body and upward and lateral injection of clastic material. Based on outcrop and subsurface studies, several potential mechanisms have been suggested for the triggering of remobilization and injection of clastic material in slope-depositional systems. In the following section, these triggering mechanisms are introduced, and their applicability to the Late Cretaceous depositional systems is discussed.

Clastic Injection Triggering Mechanisms

The mechanisms that trigger the postdepositional remobilization and injection of clastic slope systems has been the focus of much speculation. Based on seismic and core studies of Paleocene and Eocene slope-to-basin-floor systems of the United Kingdom central North Sea, three principal mechanisms have been suggested. Below, the processes associated with each of these triggering mechanisms are outlined and discussed in terms of the Upper Cretaceous clastic intrusion complexes of the Måløy slope.

1) Overpressuring: Remobilization and injection of a depositional sand body can occur if the sand body becomes so overpressured during burial that hydraulic fracturing of the top seal units occurs. One mechanism to generate overpressure in isolated slope sand bodies is by rapid burial of these units in low-permeability mudstones, such that the expulsion of pore fluids in the sand body is hindered, and overpressure is developed (see Jolly and Lonergan, 2002, for a full review). Unfortunately, the burial rate of the Upper Cretaceous depositional systems cannot be calculated based on the data presented here; thus, it is difficult to unequivocally prove clastic intrusion triggering caused by rapid burial-related overpressure development. An alternative mechanism that could cause overpressure development is the migration of hydrocarbons or formation water into the sealed sand body (Jenkins, 1930; Brooke et al., 1995; Yardley and Swarbrick, 2000; Jolly and Lonergan, 2002). In the Måløy slope study area, the flow of hydrocarbons and associated formation waters through the Upper Cretaceous succession can clearly be demonstrated. First, several exploration wells in the area have encountered oil and/or gas accumulations in Middle Jurassic Brent Group, the Upper Jurassic Viking Group, the Lower Cretaceous Rødby Formation, and the Upper Cretaceous slope fan described here. Second, seismic data indicate that all of the Upper Cretaceous sand bodies lie in the pathway between gas chimneys emanating from the underlying Upper Jurassic basins and areas of gas-triggered mud diapirism in the overlying Pliocene section (cf. Løseth et al., 2003). These observations suggest that the migration of hydrocarbons and associated formation water into the Upper Cretaceous slope sand bodies could have caused overpressure development.
2) Polygonal faulting: Seismic studies of the late Eocene Alba field, United Kingdom central North Sea, have demonstrated a close spatial correspondence between clastic dikes developed adjacent to the depositional sand body and polygonal fault systems developed in the surrounding mudstones (Lonergan and Cartwright, 1999; Cosgrove and Hillier, 2000; Gras and Cartwright, 2002; Hillier and Cosgrove, 2002). A similar spatial relationship has been observed between Paleocene and Eocene remobilized sands and polygonal faults that developed in the surrounding mud-dominated strata (Løseth et al., 2003; Huuse and Mickelson, 2004). This observation is interpreted to indicate that top seal breaching and sediment remobilization occurred because of the propagation of the polygonal faults into the overpressured sand body, with clastic material being injected up the planes of weakness represented by the faults. In the Måløy slope examples presented here, several of the channel-margin amplitude anomalies interpreted as large sandstone dikes appear to be developed along polygonal faults that developed in the surrounding mud-dominated units (Figures 6b–e, 9b). Overall, however, a lack of correspondence exists between the plan-view distribution of the interpreted clastic dikes and the polygonal faults, arguing against polygonal faulting as being the main triggering mechanism. This is discussed in detail in the following section.
3) Seismicity: Outcrop (Obermeier, 1998; Netoff, 2002) and subsurface (Jolly and Lonergan, 2002) studies suggest that fault-related, large-magnitude (i.e., magnitude 5.5–6) earthquake events may be sufficient to cause sand liquefaction, failure of the top seal unit, and the upward injection of clastic material. If preexisting planes of weakness, such as faults or fractures, are present above the remobilized unit, the injection of clastic material may preferentially

occur along these structures. When this mechanism is considered in terms of the depositional systems documented here, it is difficult to conclusively demonstrate that the Måløy slope experienced large-scale earthquake events during the Late Cretaceous. For example, minor offset of the Upper Cretaceous strata across the Gjøa fault zone suggests that this structure was reactivated some time after the Late Cretaceous, although the exact magnitude of seismic events associated with this fault movement is unknown. It is similarly difficult to establish the exact timing of activity on and the magnitude of earthquakes associated with the large-displacement (>5-km; >3-mi) Øygården fault zone, located 20 km (12 mi) to the east of the Upper Cretaceous slope systems. The trenching of Holocene and Pleistocene clastic intrusions provides evidence to suggest that earthquakes, regardless of their magnitude, could not have been a major factor in the remobilization and injection of the Late Cretaceous sands. For example, these studies indicate that because of overburden pressure, it is difficult to liquefy sands by seismic activity at burial depths greater than 10 m (33 ft) (Obermeier, 1998). Some of the interpreted clastic dikes adjacent to the Late Cretaceous depositional systems have compacted heights of 100 ms (or approximately 100 m [330 ft]), indicating that the primary depositional sand body was buried to this depth or greater before injection occurred, an order of magnitude greater than that considered the maximum for seismically driven sand remobilization and injection. This implies that even the largest magnitude events could not have triggered remobilization and injection.

Controls on Clastic Injection Complex Geometry and Distribution

A model to account for the cross section and plan-view geometry and distribution of the clastic intrusion complexes adjacent to the Late Cretaceous slope-depositional systems has to consider the following observations:

- the development of the largest clastic dikes at the margins of the depositional system from which they are sourced
- the elongate alignment of channel-margin clastic dikes along the slope channels
- the preferential alignment of clastic dikes parallel to the margins of the slope channel where they are developed above the channel axes
- the occasional spatial relationship between clastic dikes and polygonal faults developed in the encasing mud-dominated strata

As discussed in the previous section, polygonal faults developing in the mudstones sealing the overpressured slope sand bodies may propagate into the sand bodies and trigger remobilization and injection (Lonergan and Cartwright, 1999; Lonergan et al., 2000; Gras and Cartwright, 2002; Molyneux et al., 2002) (Figure 13b). In this case, upward injection will preferentially occur along the fault planes; thus, clastic dikes would display a polygonal distribution in plan view. In cross section, some of the interpreted clastic dikes described in this study do appear to occur along offsets associated with polygonal faults (Figure 6d, e). In plan view, however, it is clear that the clastic dikes do not display a polygonal distribution, but are elongate along the flanks of the slope channels from which they are sourced. Furthermore, it is commonly observed that the clastic dikes are offset by the polygonal faults, indicating that the formation of the clastic intrusions occurred before the formation of the polygonal faults. Taken together, the lack of correspondence between the spatial distribution of the clastic dikes and the polygonal faults and the apparent difference in the timing of formation of the two structures suggests that polygonal faults were not the key control on the triggering, geometry, and distribution of the clastic injections.

As discussed previously, most of the clastic injections occur at the margins of the depositional systems from which they were sourced. In particular, in the case of the largest clastic dikes, these features are elongated along the margins of the slope channels or the slope fan (Figures 6b–e, 8, 10–12). A similar spatial relationship between the main depositional sand body and channel-margin clastic dikes is observed in the upper Eocene Alba field of the United Kingdom central North Sea (Lonergan and Cartwright, 1999; Cosgrove and Hillier, 2000). Although it has previously been suggested that polygonal faulting in mudstones encasing the main depositional sand body triggered remobilization and injection and the subsequent distribution of the clastic dikes, an alternative model involving differential compaction and forced folding has been suggested, which may apply to the Upper Cretaceous example presented here (Figure 14). In this model, it is suggested that differential compaction adjacent to the main depositional sand body would result in the formation of zones of maximum extensional strain at the margins of the slope channel sand bodies. Small-scale faults and fractures that strike parallel to the margins of the channels develop in the zones of maximum extensional strain, and clastic material is injected up these zones of weakness to form winglike clastic dikes that flank the channels (Cosgrove and Hillier, 2000; Hillier and Cosgrove, 2002). This is an attractive model for the formation of the clastic injection complexes described in this chapter because seismic sections clearly indicate that differential compaction occurred adjacent

to the slope-depositional sand bodies, and that the largest clastic dikes typically flank the margins of the depositional sand body with which they are associated (Figure 14).

Clastic sills are spatially related to clastic dikes, occurring either halfway along the clastic dikes emanating from the channel margins approximately 75 ms above the channel base or at the uppermost tips of the clastic dikes (Figure 6b–e). The consistent development of large clastic sills at a horizon 75 ms above the interpreted channel base may suggest that this horizon represented a mechanically weak unit along which clastic sills propagated during injection. One potential model that could account for the development of clastic sills at the upper tips of clastic dikes comes from studies of clastic intrusion complexes in the Balder Formation in the south Viking graben. In this model, the occurrence of clastic sills at the upper tips of clastic dikes coincide with basin-scale unconformities, leading to the suggestion that the clastic sills formed as extrusive features at the contemporary sea floor (Hurst et al., 2003; Huuse et al., 2003, 2004). Within the Måløy slope area, no significant unconformities are recorded in the Upper Cretaceous; thus, it is interpreted that the Upper Cretaceous clastic sills described here are unlikely to have formed as extrusive sea-floor features. Alternatively, the development of clastic sills at the upper tips of clastic dikes, a relationship that is commonly observed in clastic injection complexes, may simply reflect the depth at which the fluid pressure exceeds the maximum overburden pressure, and clastic intrusions can no longer propagate across bedding in the form of dikes; thus, they evolve into sills and propagate parallel to bedding (Jolly and Lonergan, 2002).

IMPLICATIONS OF CLASTIC REMOBILIZATION AND INJECTION FOR EXPLORATION AND PRODUCTION

The remobilization and injection of deep-water depositional sand bodies at a variety of scales has important implications for the exploration and production of hydrocarbons contained in such units (see summary in Lonergan et al., 2000). Although not typically deliberately targeted during exploration drillings, clastic intrusion complexes, depending on their scale, represent an exploration target themselves, especially in cases where the depositional sand body is in the mature stages of development. For example, several wells in the Eocene Alba field United Kingdom central North Sea have demonstrated that amplitude anomalies that developed at the margins of the main submarine channel are the seismic response of 20-m (66-ft)-thick, hydrocarbon-bearing clastic dikes. Furthermore, several wells typically targeting deeper reservoir sand bodies have demonstrated that V-shaped amplitude anomalies (V-brights of Løseth et al., 2003) in the Eocene and Paleocene are the seismic response of sand-rich (net to gross about 100%) clastic injections as much as 65 m (213 ft) thick (Molyneux et al., 2002; Løseth et al., 2003; Huuse and Mickelson, 2004). The amplitude anomalies interpreted as clastic intrusions in this study are of a comparable scale to those documented in both the examples given above. For example, the largest, most laterally continuous clastic dikes developed adjacent to the Upper Cretaceous slope channels are 20–30 m (66–98 ft) thick (assuming the upper trough event and lower peak event are the seismic response of the top and base of the sand, respectively), as much as 100 m (330 ft) high, and extend more or less continuously for more than 15 km (9 mi) along the lengths of the channels. Assuming that the clastic intrusion complexes have a net to gross of almost 100%, as exemplified by most of the clastic injection features that penetrated in the northern North Sea, this gives a potential reservoir volume of 4.75×107 m^3 (1.54×109 ft^3) for an individual channel-margin wing complex. Clastic intrusion complexes located above the axes of depositional systems, although typically smaller and more locally developed than those at the margins of the depositional systems, may also contain exploitable volumes.

Regarding the implications for production of hydrocarbons, previous studies have indicated that remobilization and injection of slope sand bodies can cause modification of the overall reservoir geometry and volumetrics, changes in reservoir properties, changes in top reservoir structuration, and enhanced connectivity between isolated sand bodies (see review in Lonergan et al., 2000). In the examples presented here, remobilization and injection, in addition to differential compaction, have clearly altered the potential reservoir geometry. For example, remobilization and injection have given the depositional units their distinctive wings, whereas differential compaction, intimately linked to the remobilization and injection process, has given channel A its distinct mounded geometry (Figures 6b–d, 8, 9, 12). The structure of the top sand body surface has been complicated by the development of clastic intrusions above the axes of the channels. In the case of channel A, injection above the axis has created such an undulose top surface that direct mapping of the top of the sand body is not possible over large parts of the channel (e.g., channel A; Figure 6b).

The marked changes to the depositional geometry of the sand bodies described above may cause problems when attempting to optimize production well placement. In a depositional sand body extremely modified by remobilization and injection (i.e., channel A; Figures 6b, 8, 9, 12), depending on the timing of charge

vs. intrusion development, it is possible that a part of the oil or gas column may have migrated up into, and be contained solely within, clastic intrusion complexes adjacent to the main reservoir sand body. In this situation, the clastic intrusion complexes would represent the only target. In contrast, if the clastic intrusion complexes consist of numerous, small, irregularly distributed sands, then the hydrocarbons may be distributed into numerous, laterally discontinuous, subeconomic accumulations.

CONCLUSIONS

An integrated three-dimensional seismic, well, and core study indicates the development of a series of slope channel- and fan-depositional systems in the Upper Cretaceous interval of the Måløy slope, Norwegian margin. Because of their sand content and occurrence in a mud-dominated succession, the slope-depositional systems manifest as high-amplitude reflector packages on seismic reflection data. The Upper Cretaceous depositional systems are flanked and overlain by two types of amplitude anomalies that display unusual geometries in cross section and plan view. The first type of anomaly is bedding discordant and crosscuts overlying reflections, dips 10–20°, is as much as 100 ms high, and is typically developed at the margins of the slope systems. The second type of amplitude anomaly is bedding concordant, as much as 400 m (1312 ft) long in cross section, and is developed either halfway up or at the upper tips of the bedding-discordant anomalies. In 3-D, the steeply dipping anomalies developed at the margins of the slope-depositional systems form winglike structures that are elongate along the lengths of the slope-depositional systems. Based on their close spatial relationship to the Upper Cretaceous slope-depositional systems and inferred sand content, the bedding-discordant and bedding-concordant amplitude anomalies are interpreted as clastic dikes and sills, respectively, sourced from the Upper Cretaceous slope systems. Although the mechanism that caused initial overpressuring of the sand bodies is unclear, it is speculated that a combination of the migration of basinal fluids into the sealed depositional sand bodies and the rapid burial of the sand bodies in low-permeability mudstones may have contributed. The development of the largest clastic dikes at the margins of the depositional systems suggests that differential compaction and forced folding adjacent to the buried depositional systems triggered remobilization and injection and the subsequent geometry and distribution of clastic injection features. The postdepositional remobilization and injection of clastic slope systems as exemplified in this study have important implications for hydrocarbon exploration and production in slope systems because this process has caused marked changes in primary reservoir geometry and has resulted in the development of clastic intrusions that are large enough to represent stand-alone exploration targets.

ACKNOWLEDGMENTS

Frodi Hjaltason, Ole Martinsen, Harald Flesche, Steve Corfield, Tom Dreyer, and Paul Spencer are thanked for helpful discussions during the study and during the preparation of the manuscript. Pete Rawlinson, Helge Løseth, and Joe Cartwright are thanked for their critical reviews of the manuscript. The ideas expressed in this chapter do not necessarily represent the views of Norsk Hydro ASA. Finally, Norsk Hydro ASA are thanked for their permission to publish this study.

REFERENCES CITED

Archer, J. B., 1984, Clastic intrusions in deep-sea fan deposits of the Rosroe Formation, Lower Ordovician, western Ireland: Journal of Sedimentary Petrology, v. 54, p. 1197–1205.

Bergslien, D., 2002, Balder and Jotun; two sides of the same coin? A comparison of two Tertiary oil fields in the Norwegian North Sea: Petroleum Geoscience, v. 8, p. 349–363.

Brooke, C. M., T. J. Trimble., and T. A. Mackay, 1995, Mounded shallow gas sands from the Quaternary of the North Sea: Analogues for the formation of sand mounds in deep water Tertiary sediments, *in* A. J. Hartley and D. J. Prosser, eds., Characterisation of deep-marine clastic systems: Geological Society (London) Special Publication 94, p. 95–101.

Bugge, T., B. Tveiten, and S. Backstrom, 2001, The depositional history of the Cretaceous in the northeastern North Sea, *in* O. J. Martinsen and T. Dreyer, eds., Sedimentary environments offshore Norway— Palaeozoic to Recent: Norwegian Petroleum Federation Special Publication 10, p. 279–291.

Cartwright, J. A., 1994, Episodic basin-wide fluid expulsion from geopressured shale sequences in the North Sea Basin: Geology, v. 22, p. 447–450.

Cartwright, J. A., 1996, Polygonal fault systems: A new type of fault system revealed by 3-D seismic data from the North Sea Basin, *in* P. Weimer and T. L. Davis, eds., Applications of 3-D seismic data to exploration and production: AAPG Studies in Geology 42, p. 225–230.

Cartwright, J. A., and L. Lonergan, 1996, Volumetric contraction during the compaction of mudrocks: A mechanism for the development of regional-scale polygonal fault systems: Basin Research, v. 8, p. 183–193.

Cosgrove, J. W., and R. D. Hillier, 2000, Forced fold development within Tertiary sediments of the Alba field, UKCS: Evidence of differential compaction and post-depositional sandstone remobilisation, *in* J. W.

Cosgrove and M. S. Ameen, eds., Forced folds and fractures: Geological Society (London) Special Publication 169, p. 61–71.

Dewhurst, D. N., J. A. Cartwright, and L. Lonergan, 1999, The development of polygonal fault systems by syneresis of colloidal sediments: Marine and Petroleum Geology, v. 16, p. 793–810.

Dixon, R. J., K. Schofield, R. Anderton, A. D. Reynolds, R. W. S. Alexander, M. C. Williams, and K. G. Davies, 1995, Sandstone diapirism and clastic intrusion in the Tertiary submarine fans of the Bruce-Beryl Embayment, Quadrant 9, UKCS, *in* A. J. Hartley and D. J. Prosser, eds., Characterisation of deep-marine clastic systems: Geological Society (London) Special Publication 94, p. 77–94.

Duranti, D., A. Hurst, C. Bell, S. Groves, and R. Hanson, 2002, Injected and remobilized sands from the Alba field (Eocene, UKCS): Core and wireline characteristics: Petroleum Geoscience, v. 8, p. 99–107.

Fraser, S. I., A. M. Robinson, H. D. Johnson, J. R. Underhill, D. Kadolsky, R. Connell, P. Johannessen, and R. Ravnås, 2003, Upper Jurassic, *in* D. E. Evans, C. Graham, A. Armour, and P. Bathurst, eds., The millenium atlas: Petroleum geology of the central and northern North Sea: Geological Society (London), p. 372–437.

Gabrielsen, R. H., R. Kyrkjebø, J. I. Faleide, W. Fjeldskaar, and T. Kjennerud, 2001, The Cretaceous post-rift basin configuration of the northern North Sea: Petroleum Geoscience, v. 7, p. 137–154.

Gras, R., and J. Cartwright, 2002, Tornado faults: The seismic expression of the early Tertiary on PS-data, Chestnut field, North Sea: 64th European Association of Geoscientists and Engineers Conference and Exhibition, Florence, Extended Abstracts, H020.

Guargena, C. G., G. B. Smith, J. Wardell, T. H. Nilsen, and T. M. Hegre, 2002, Sand injections at Jotun field, North Sea— Their possible impact on recoverable reserves: 64th European Association of Geoscientists and Engineers Conference and Exhibition, Florence, Extended Abstracts, H018.

Hillier, R. D., and J. W. Cosgrove, 2002, Core and seismic observations of overpressure-related deformation within Eocene sediments of the outer Moray Firth, UKCS: Petroleum Geoscience, v. 8, p. 141–149.

Hiscott, R. N., 1979, Clastic sills and dykes associated with deep-water sandstones, Tourelle Formation, Ordovician Quebec: Journal of Sedimentary Petrology, v. 49, p. 1–10.

Hurst, A., J. Cartwright, M. Huuse, R. Jonk, A. Schwab, D. Duranti, and B. Cronin, 2003, Significance of large-scale sand injectites as long-term fluid conduits: Evidence from seismic data: Geofluids, v. 3, p. 263–274.

Huuse, M., and M. Mickelson, 2004, Eocene sandstone intrusions in the Tampen Spur area (Norwegian North Sea Quad 34) imaged by 3D seismic data: Marine and Petroleum Geology, v. 21, p. 141–155.

Huuse, M., D. Duranti, C. G. Guargena, P. Prat, K. Holm, N. Steinsland, B. T. Cronin, A. Hurst, and J. Cartwright, 2003, Sandstone intrusions: Detection and significance for exploration and production: First Break, v. 21, p. 33–42.

Huuse, M., D. Duranti, D. N. Steinsland, C. G. Guergena, P. Prat, K. Holm, J. A. Cartwright, and A. Hurst, 2004, Seismic characteristics of large-scale sandstone intrusions in the Paleogene of the south Viking graben, UK and Norwegian North Sea, *in* R. Davies, J. Cartwright, S. A. Stewart, J. R. Underhill, and M. Lappin, eds., 3D seismic technology: Application to the exploration of sedimentary basins: Geological Society (London) Memoir 29, p. 257–271.

Jenkins, O., 1930, Sandstone dikes as conduits for oil migration through shales: AAPG Bulletin, v. 14, p. 411–421.

Jenssen, A. I., D. Bergslian, M. Rye-Larsen, and R. M. Lindholm, 1993, Origin of complex mound geometry of Paleocene submarine-fan sandstone reservoirs, Balder field, Norway, *in* J. R. Parker, ed., Petroleum geology of northwest Europe: Proceedings of the 4th Conference: Geological Society (London), p. 135–143.

Jolly, R. J. H., and L. Lonergan, 2002, Mechanisms and controls on the formation of sand intrusions: Journal of the Geological Society (London), v. 159, p. 605–617.

Lonergan, L., and J. Cartwright, 1999, Polygonal faults and their influence on deep-water sandstone reservoir geometries, Alba field, United Kingdom central North Sea: AAPG Bulletin, v. 83, p. 410–432.

Lonergan, L., N. Lee, H. D. Johnson, R. J. H. Jolly, and J. Cartwright, 2000, Remobilisation and injection in deepwater depositional systems: Implications for reservoir architecture and prediction, *in* P. Weimer, R. M. Slatt, J. Coleman, N. C. Rosen, H. Nelson, A. H. Bouma, M. J. Styzen, and D. T. Lawrence, eds., Deep water reservoirs of the world: Gulf Coast Section SEPM Foundation 20th Annual Conference, p. 515–532.

Løseth, H., L. Wensaas, B. Arntsen, and M. Hovland, 2003, Gas and fluid injection triggering shallow mud mobilization in the Hordaland Group, North Sea, *in* P. Rensbergen, R. van Hillis, A. Maltman, and C. K. Morley, eds., Subsurface sediment mobilization: Geological Society (London) Special Publication 216, p. 139–157.

MacLeod, M. K., R. A. Hanson, C. R. Bell., and S. McHugo, 1999, The Alba field ocean bottom cable seismic survey: Impact on development: The Leading Edge, v. 18, p. 1306–1312.

Martinsen, O. J., F. Bøen, M. A. Charnock, G. Mangerud, and A. Nøttvedt, 1999, Cenozoic development of the Norwegian margin: Sequences and sedimentary response to variable basin physiography and tectonic setting, *in* A. J. Fleet and S. A. R. Boldy, eds., Petroleum geology of northwest Europe: Proceedings of the 5th Conference: Geological Society (London), p. 293–304.

Martinsen, O. J., T. Lien, and C. A. L. Jackson, 2005, Cretaceous and Paleogene turbidite systems in the North Sea and Norwegian Sea basins: Source, staging area and basin physiography controls on reservoir development, *in* A. G. Dore and B. Vining, eds., Petroleum geology of northwest Europe and global perspectives: Proceedings of the 6th Petroleum Geology Conference: Geological Society (London), p. 1147–1164.

Mayall, M., and I. Stewart, 2000, The architecture of turbidite slope channels, *in* P. Weimer, R. M. Slatt, J. Coleman, N. C. Rosen, H. Nelson, A. H. Bouma, M. J. Styzen, and D. T. Lawrence, eds., Deep water reservoirs of the world: Gulf Coast Section SEPM Foundation 20th Annual Conference, p. 578–586.

Molyneux, S., J. Cartwright, and L. Lonergan, 2002, Conical sandstone injection structures imaged by 3D seismic in the central North Sea, UK: First Break, v. 20, p. 383–393.

Netoff, D., 2002, Seismogenically induced fluidisation of Jurassic erg sands, south-central Utah: Sedimentology, v. 49, p. 65–80.

Obermeier, S. F., 1998, Liquefaction evidence for strong earthquakes of Holocene and latest Pleistocene ages in the states of Indiana and Illinois, U.S.A.: Engineering Geology, v. 50, p. 227–254.

Prather, B. E., F. B. Keller, and M. A. Chapin, 2000, Hierarchy of deep-water architectural elements with reference to seismic resolution: Implications for reservoir prediction and modelling, *in* P. Weimer, R. M. Slatt, J. Coleman, N. C. Rosen, H. Nelson, A. H. Bouma, M. J. Styzen, and D. T. Lawrence, eds., Deep water reservoirs of the world: Gulf Coast Section SEPM Foundation 20th Annual Conference, p. 817–835.

Purvis, K., J. Kao, K. Flanagan, J. Henderson, and D. Duranti, 2002, Complex reservoir geometries in a deep water clastic sequence, Gryphon field UKCS: Injection structures, geological modeling and reservoir simulation: Marine and Petroleum Geology, v. 19, p. 161–179.

Shoulders, S. J., and J. A. Cartwright, 2004, Constraining the depth and timing of large-scale conical sandstone intrusions: Geology, v. 32, p. 661–664.

St. J. Newman, M., M. L. Reeder, A. H. W. Woodruff, and I. R. Hatton, 1993, The geology of the Gryphon oil field, *in* J. R. Parker, ed., Petroleum geology of northwest Europe: Proceedings of the 4th Conference: Geological Society (London), p. 123–133.

Timbrell, G., 1993, Sandstone architecture of the Balder Formation depositional system, UK Quadrant 9 and adjacent areas, *in* J. R. Parker, ed., Petroleum geology of northwest Europe: Proceedings of the 4th Conference: Geological Society (London), p. 107–121.

Yardley, G. S., and R. E. Swarbrick, 2000, Lateral transfer: A source of additional overpressure?: Marine and Petroleum Geology, v. 17, p. 523–537.

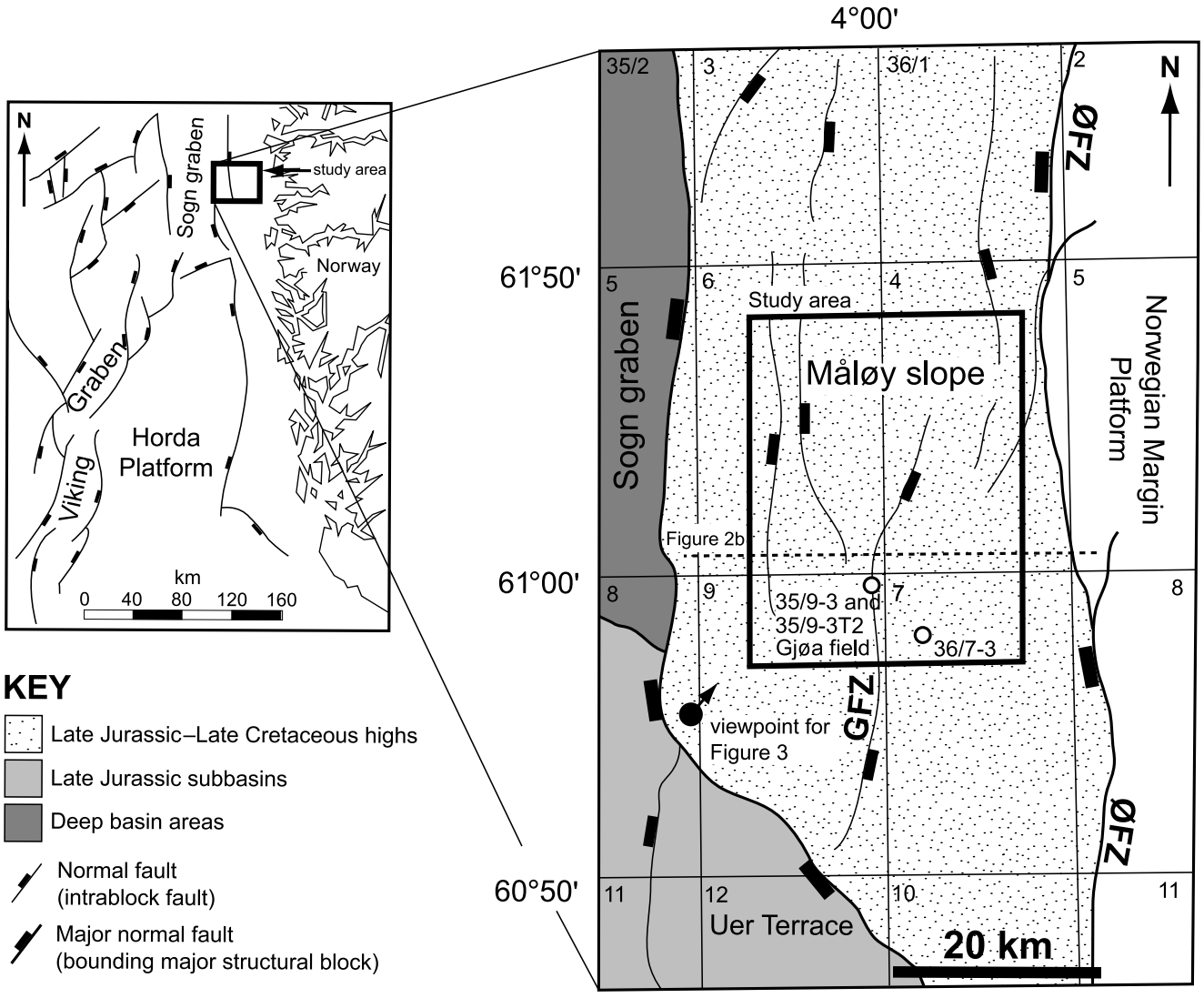

FIGURE 1. Simplified structural map of the Måløy slope area illustrating some of the main Jurassic rift-related extensional faults and the three main structural compartments associated with them. See the text for full discussion. The location of the study area shown in Figure 3 is boxed, and the location of subregional line illustrated in Figure 2b is marked. GFZ = Gjøa fault zone; ØFZ = Øygården fault zone.

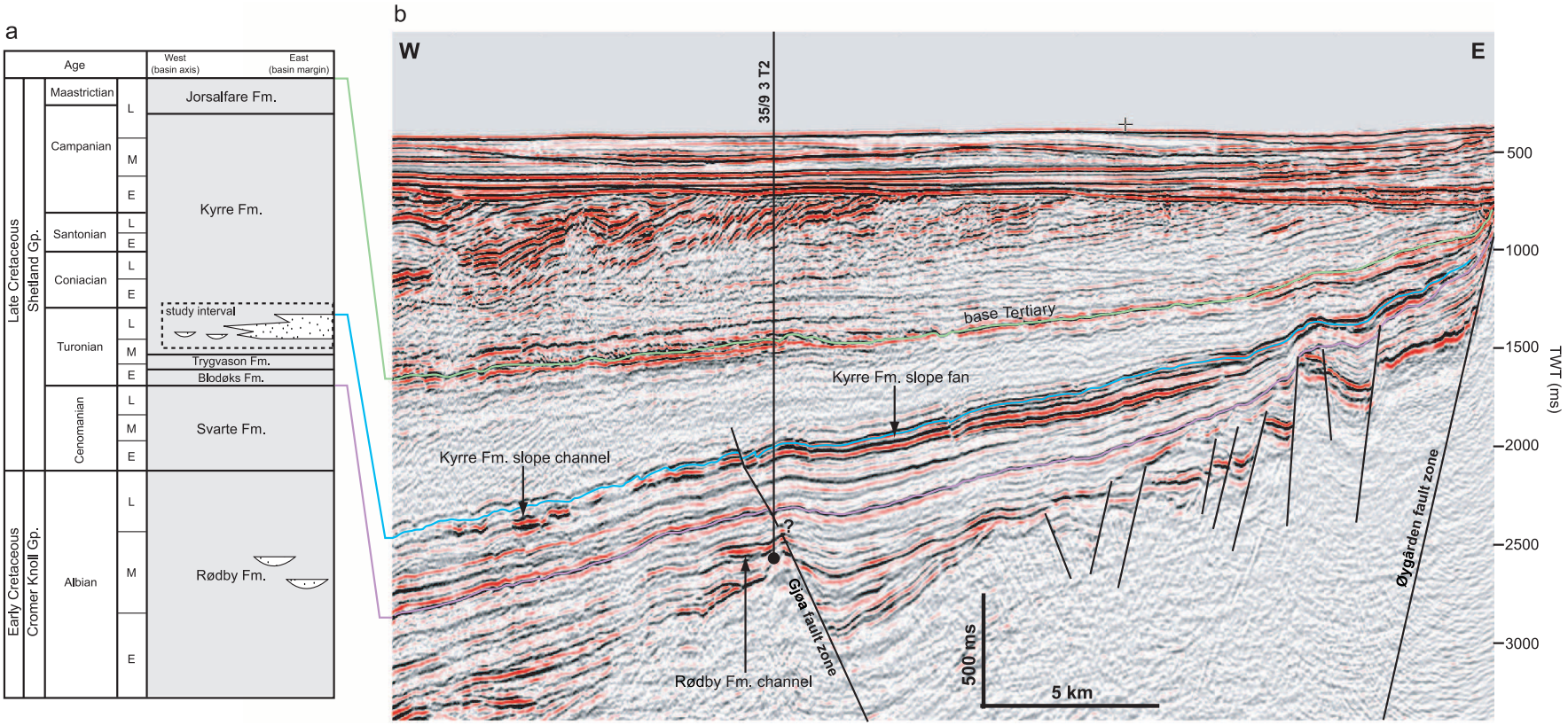

FIGURE 2. (a) Simplified stratigraphic section through the Lower and Upper Cretaceous strata of the Måløy slope. Note the mud-dominated nature of the succession (gray) and the development of submarine fans and isolated submarine channels of middle Albian (Rødby Formation), and late Coniacian–early Santonian (Kyrre Formation) age (stippled). These depositional systems were sourced from the Norwegian margin hinterland to the east. (b) Seismic line across the Måløy slope illustrating the structural setting of the Upper Cretaceous depositional systems. Note the presence of amplitude anomalies in the Upper Cretaceous Kyrre Formation and the Upper Jurassic–Lower Cretaceous faults that die out below the base of the Blodøks Formation seismic horizon. Three seismic horizons are marked; base of Blodøks Formation (purple), near-top Kyrre Sand (blue), and base Tertiary (green), marked on the stratigraphic section (b). The location of the line is shown in Figure 1. TWT = two-way traveltime.

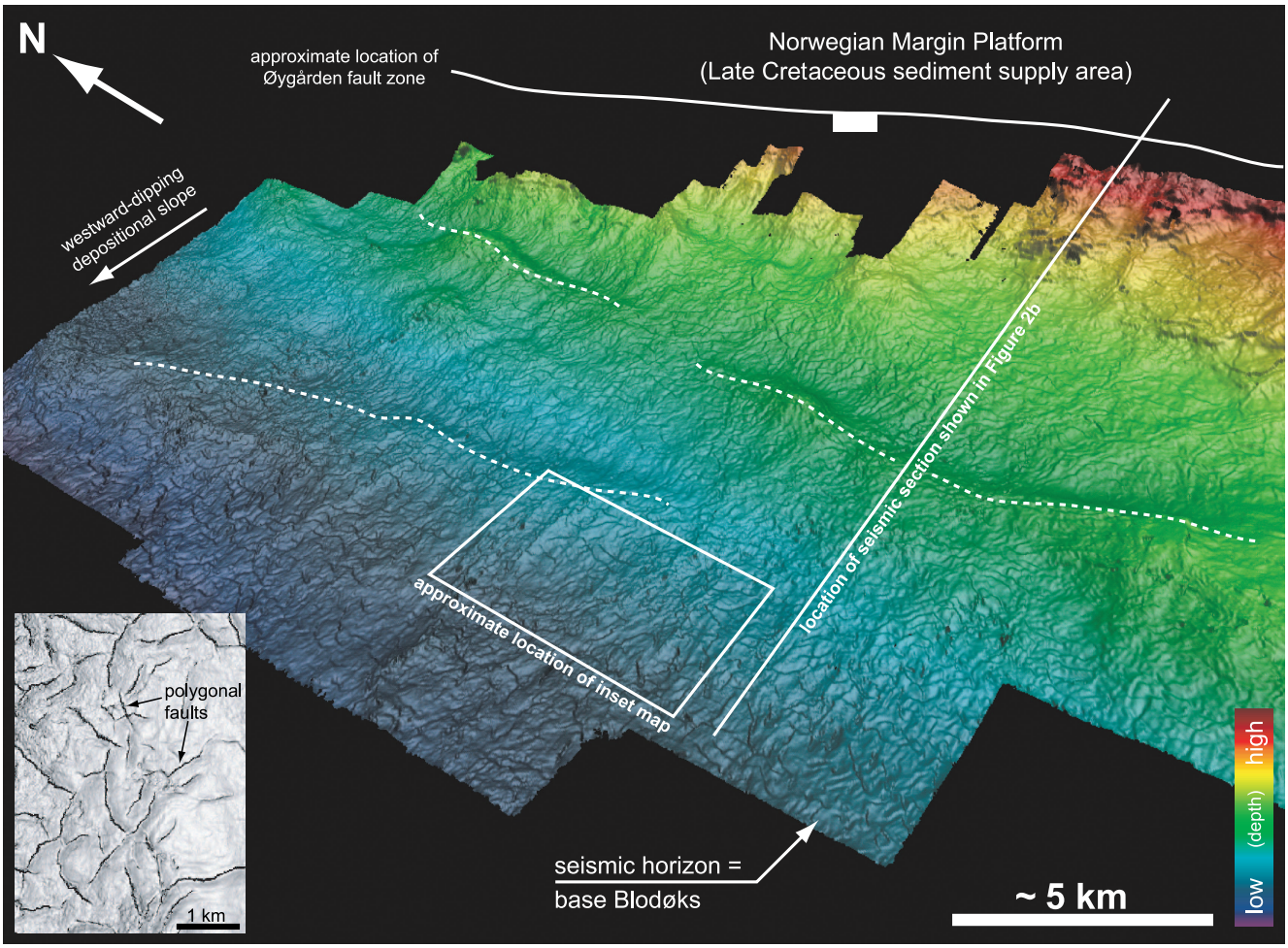

FIGURE 3. Time structure map based on 3-D mapping of the base Blodøks Formation seismic horizon. Although slightly older (i.e., early Turonian) than the late Coniacian–early Santonian deep-marine systems of interest (see Figure 2b), fault offsets indicate that only minor tectonism was experienced between the two periods; thus, the westward-dipping surface may be considered an approximation of the paleogeographic setting of the Måløy slope during the deposition of these units. Note the development of a series of north–south-trending low-relief monoclines (dashed white lines), and the polygonal fault network. The inset is a time dip map of the base Blodøks Formation seismic horizon illustrating the details of the polygonal fault network. See Figure 1 for location.

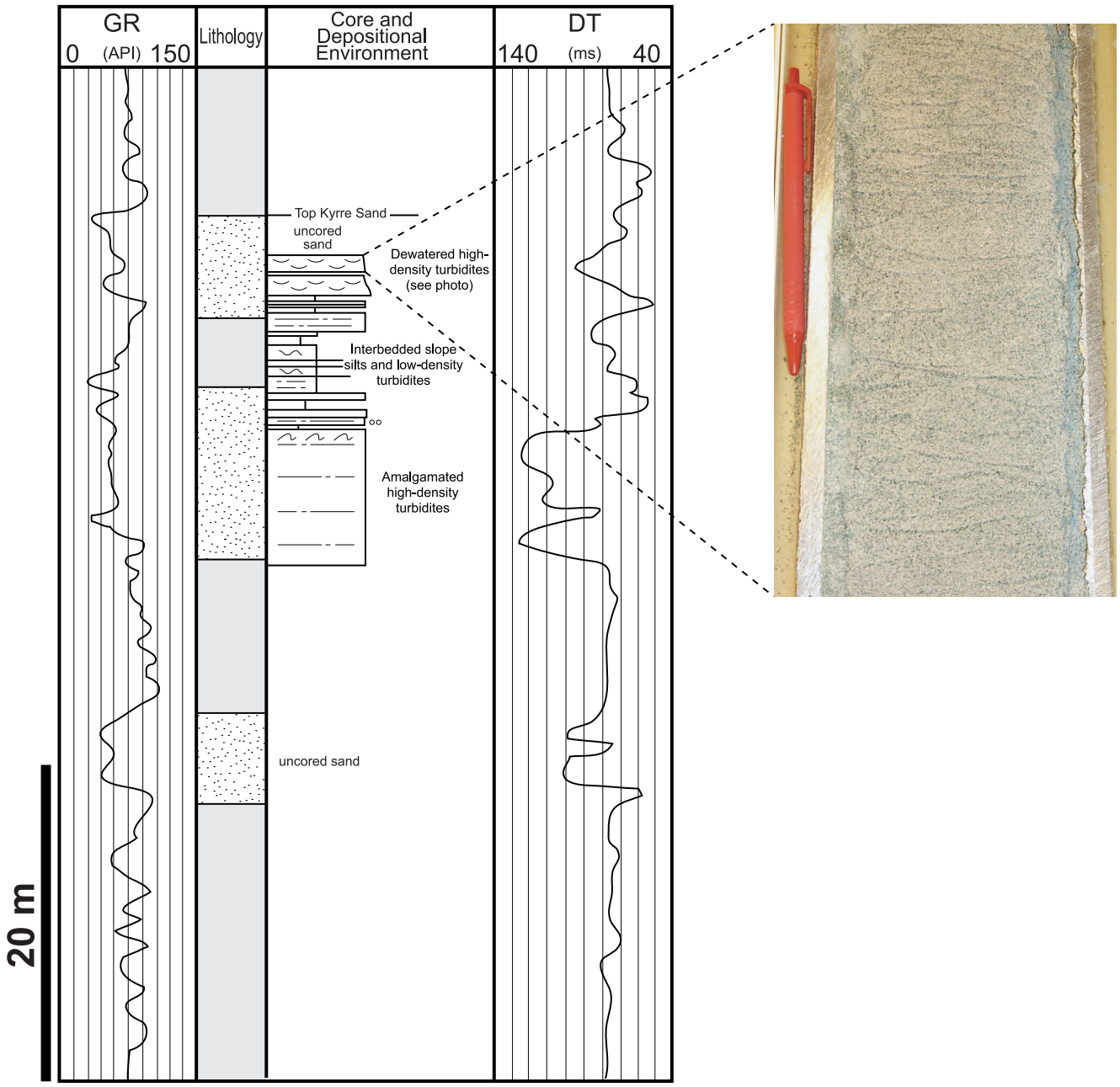

FIGURE 4. Core data from the 35/9-3 T2 illustrating the development of turbidite sands in the upper Coniacian–lower Santonian interval of the Kyrre Formation. The sands are encased within low-permeability mudstones. The photograph illustrates the dish structures developed toward the top of the sand-bearing interval. GR = gamma ray; DT = sonic velocity.

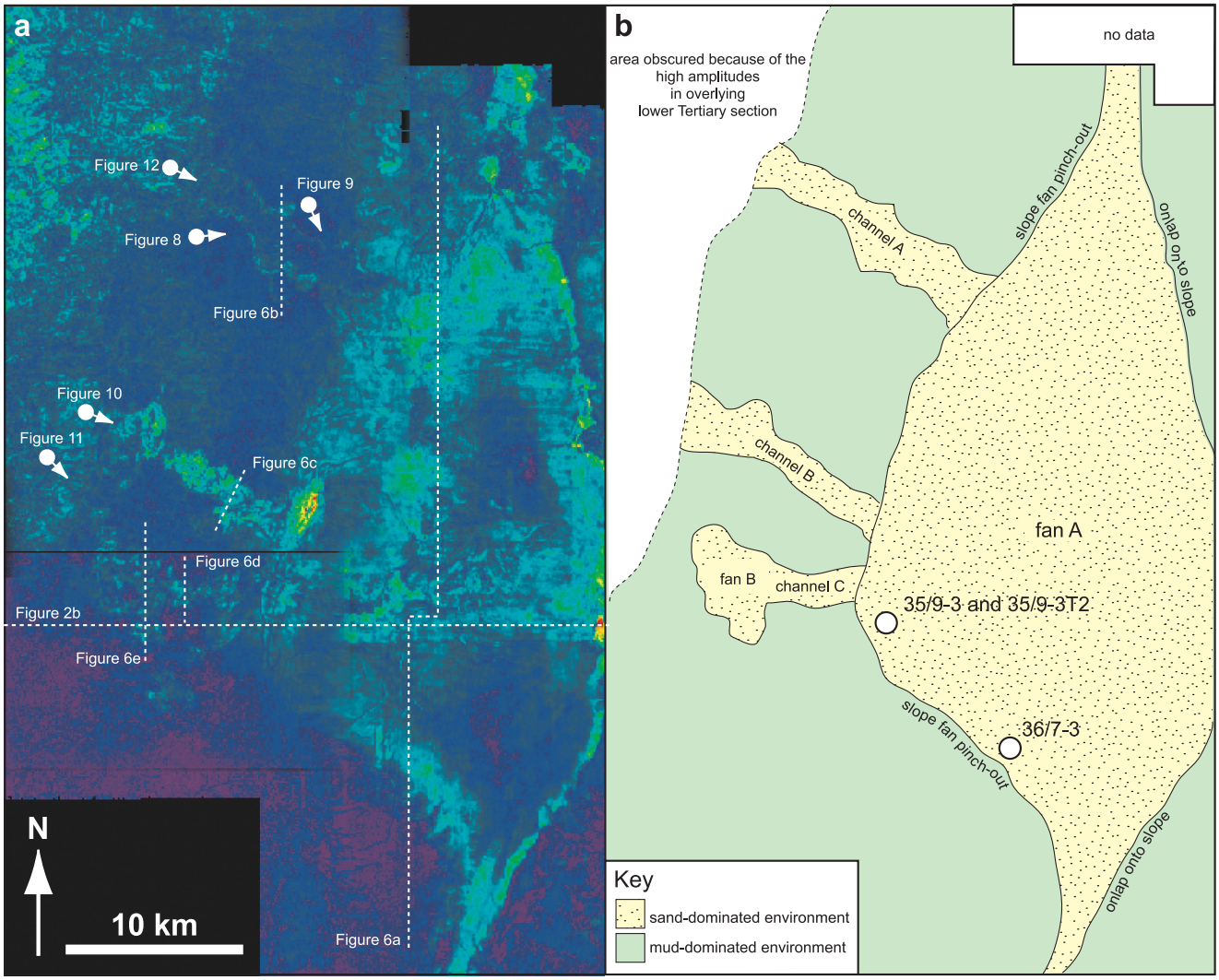

FIGURE 5. (a) Reflection strength amplitude map extracted 285 ms above the base Blodøks Formation seismic horizon (see Figure 2b) illustrating the geometry and distribution of Upper Cretaceous depositional systems on the Måløy slope. The locations of seismic lines illustrated in Figures 2b, 6a–e, 8, and 10–12 are shown. (b) Geological interpretation of the integrated reflection strength amplitude map shown in (a). See text for full discussion. The locations of wells used in this study (35/9-3, 35/9-3 T2 and 36/7-3) are shown.

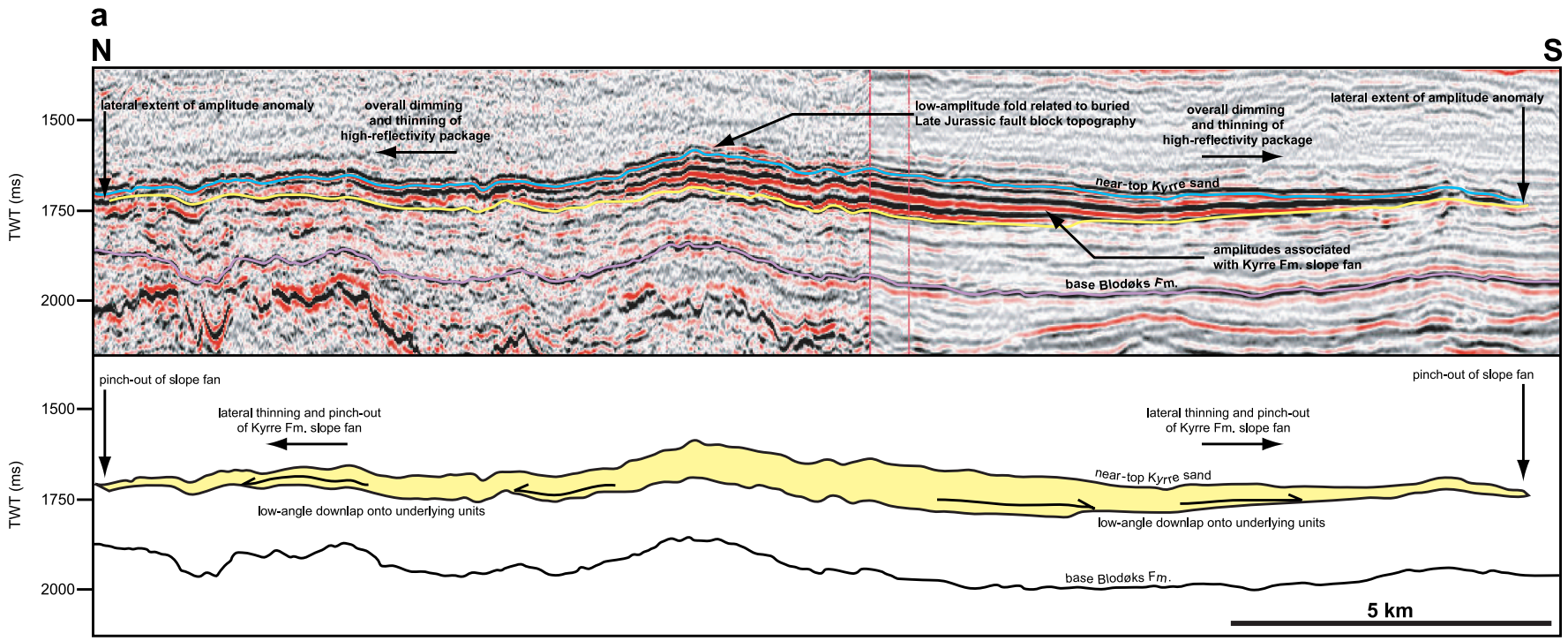

FIGURE 6. Seismic sections across five of the studied Upper Cretaceous Kyrre Formation depositional systems; (a) submarine slope fan, (b) channel A, (c) channel B, (d) channel C, and (e) terminal fan. Interpretive geological line drawings are provided for Figure 6a–e. The bedding-discordant wings and bedding-concordant amplitude anomalies developed adjacent to the submarine channels (b–d) and the terminal fan (e) are interpreted as clastic dikes and clastic sills, respectively. The locations of the seismic section are shown in Figure 5. The location of Figure 6e is also indicated in Figure 11. TWT = two-way traveltime.

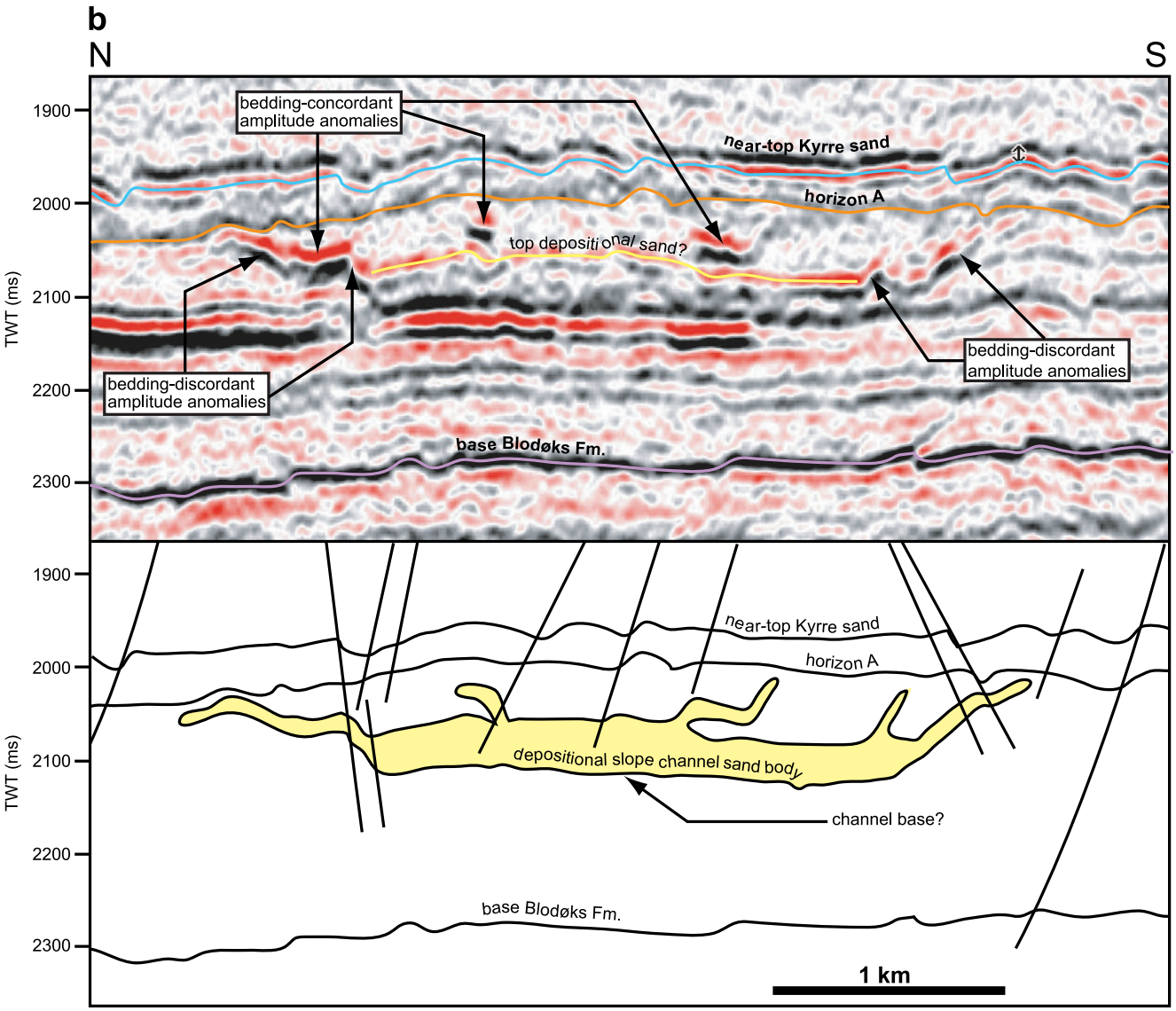

FIGURE 6. (cont.).

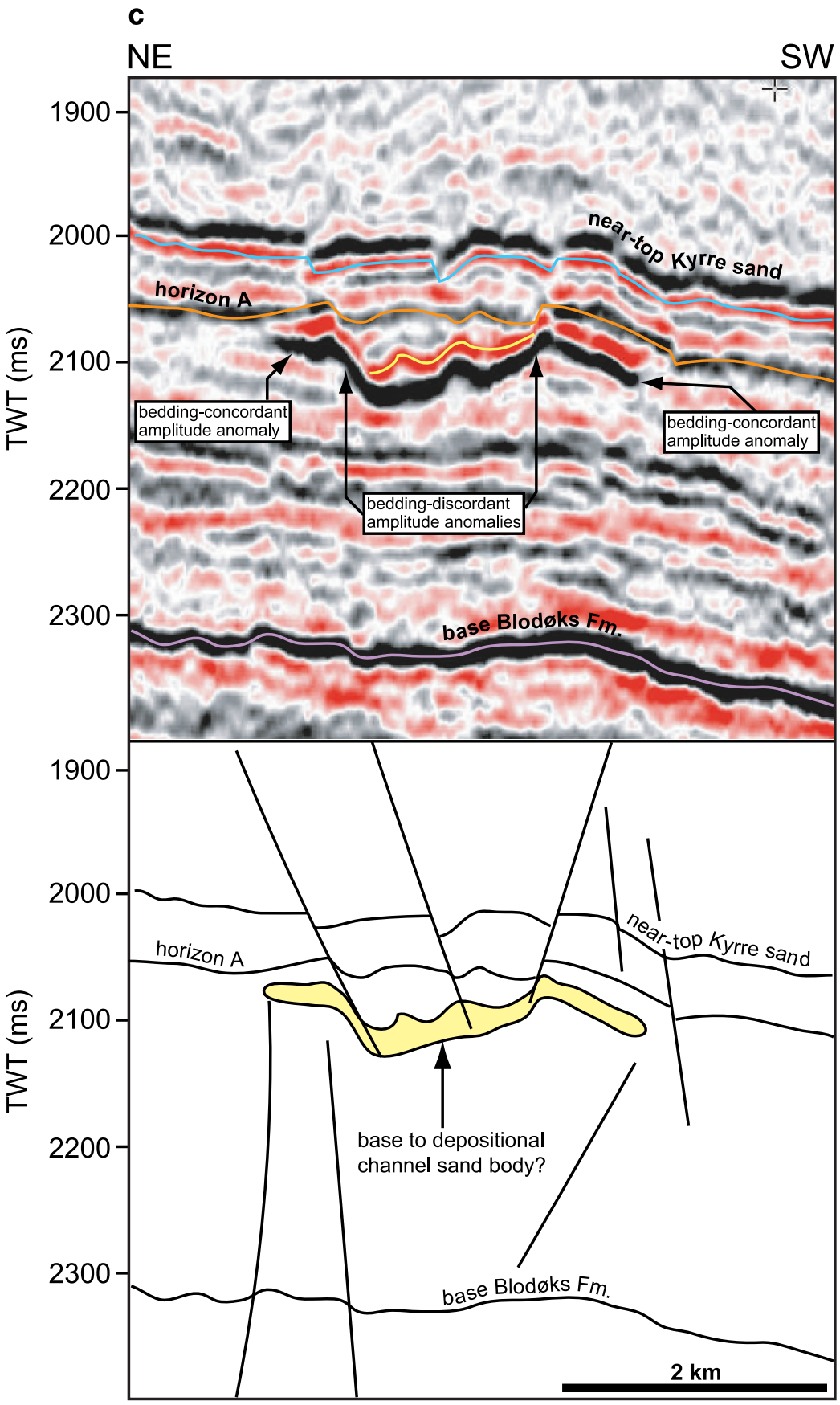

Figure 6. (cont.).

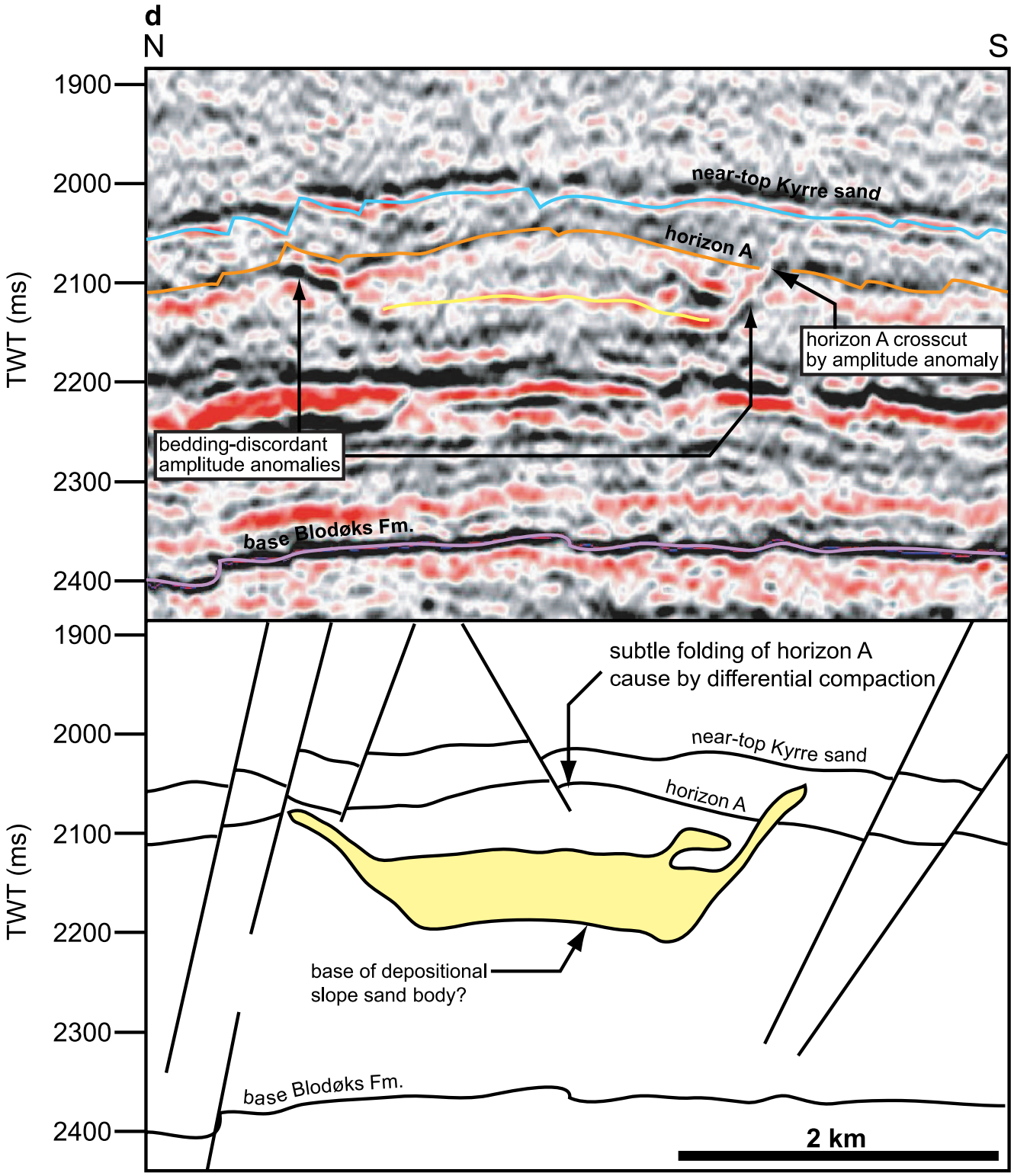

FIGURE 6. (cont.).

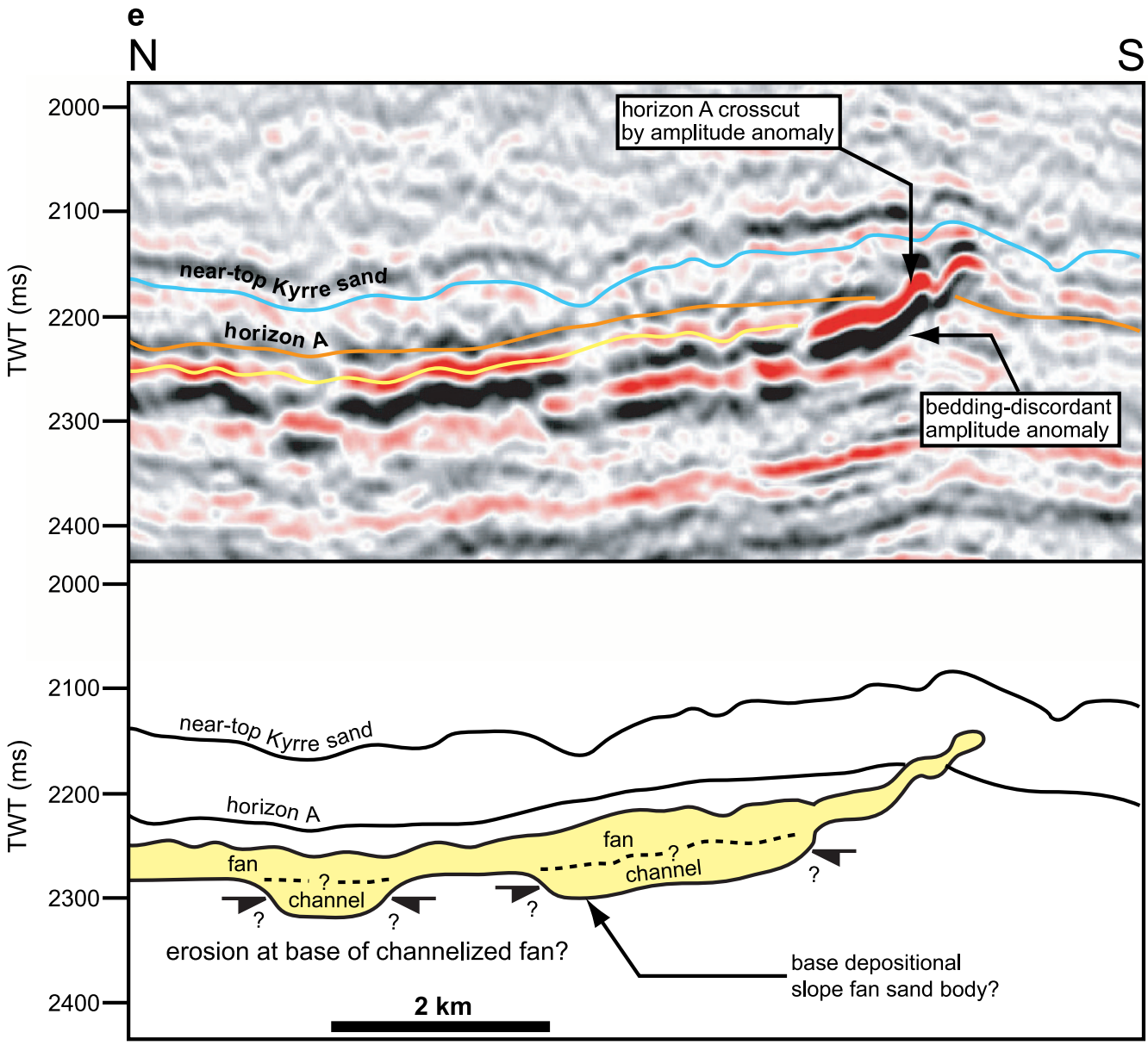

FIGURE 6. (cont.).

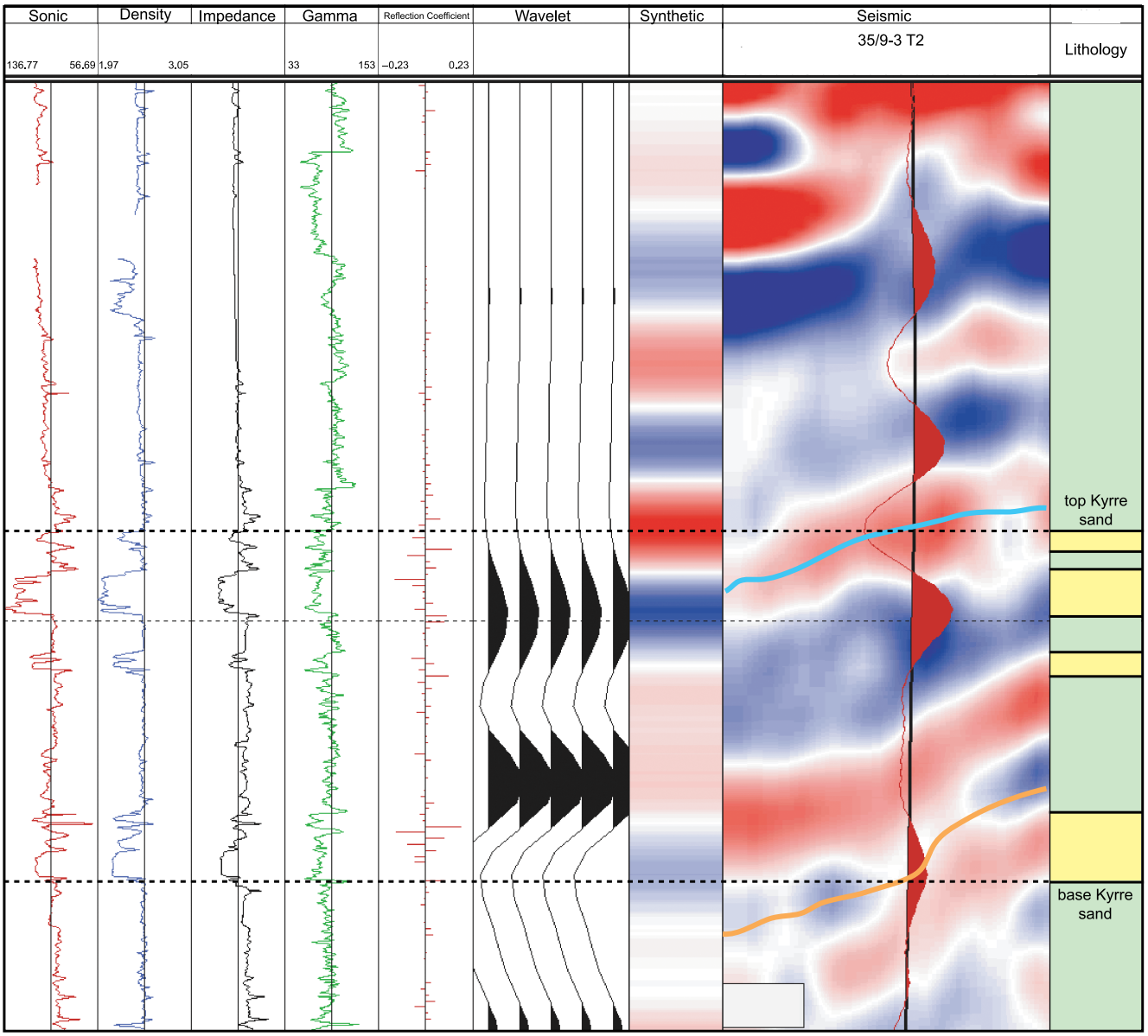

FIGURE 7. Synthetic seismograph for well 35/9-3 T2. Low-impedance, gas-bearing sands in the Kyrre Formation produce a strong negative (trough) top-sand response. At the base of the sand-bearing interval in the Kyrre Formation, a transition into mudstones marks an increase in acoustic impedance defined by a moderate amplitude positive (peak) seismic event.

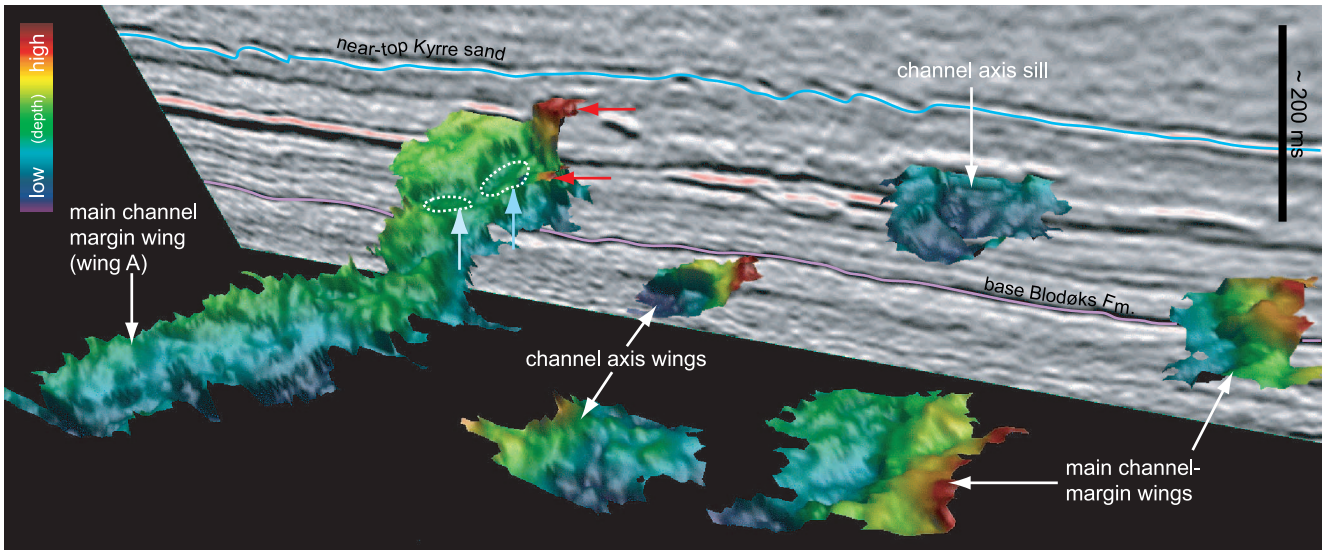

FIGURE 8. Perspective view illustrating the geometry and distribution of wing features at the margins and above the axis of channel A. Complex geometries are observed along the northern flank of the channel with two small wings (arrowed red) branching off the main channel wing. The small flat-lying, plateau areas (arrowed blue) developed along the wing are interpreted as the bedding-concordant sill component of the channel-margin injection complex. Simple, planar geometries characterize the wings developed along the southern margin of the channel and above the channel axis. The large, flat-lying amplitude anomaly developed above the channel axis is interpreted as an injected clastic sill. For location of viewpoint, see Figure 5a.

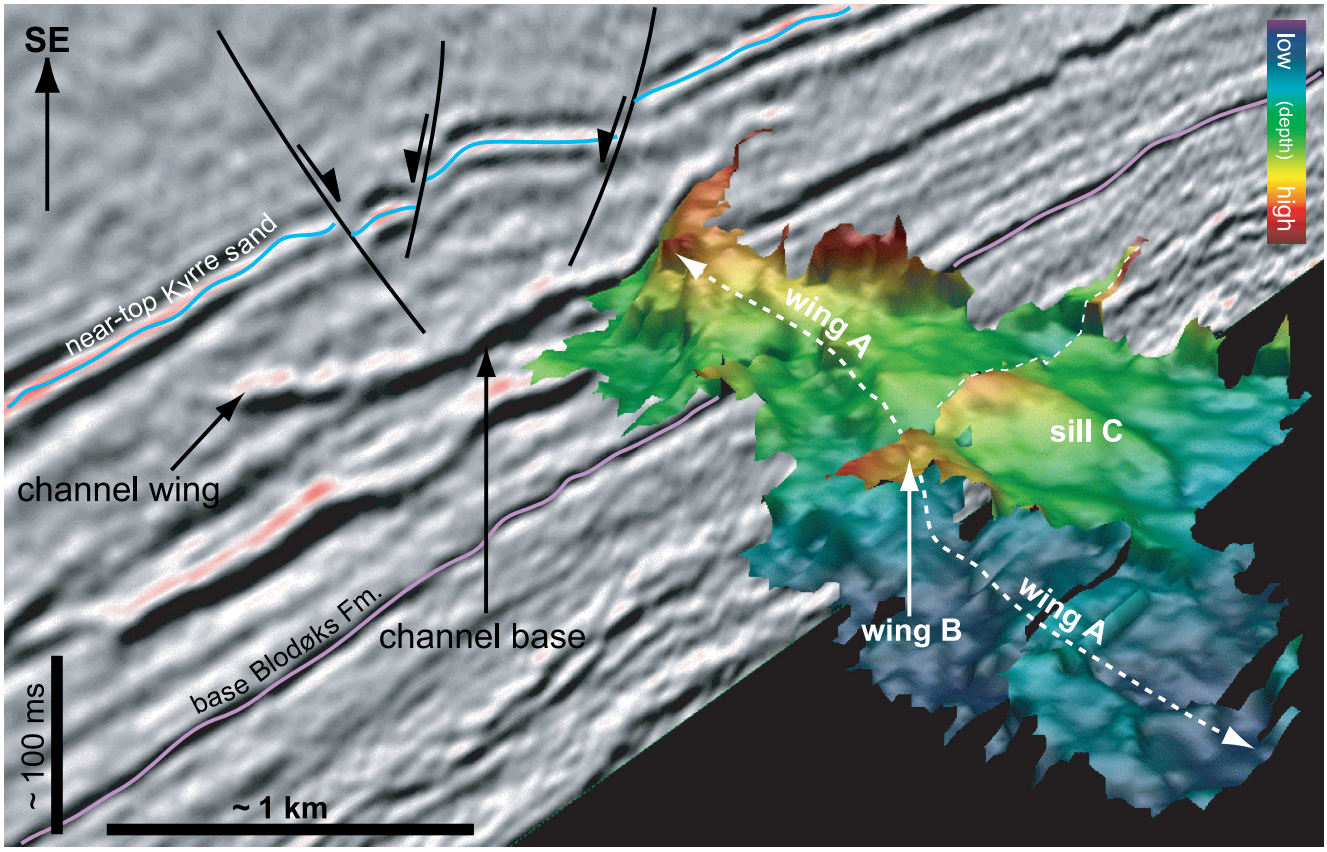

FIGURE 9. Perspective view of the southern margin of channel A illustrating the 3-D geometrical complexity of channel-margin wing complexes. In the center of the image, the main wing (wing A) is relatively planar, developing into a sill (sill C) at its upper tip to the right of the image. A smaller wing feature (wing B) branches off wing A, cutting upward through the overlying strata toward the axis of the channel. A similar (unmapped) laterally continuous wing feature is also developed along the northern margin of the channel. Location of viewpoint is shown in Figure 5a.

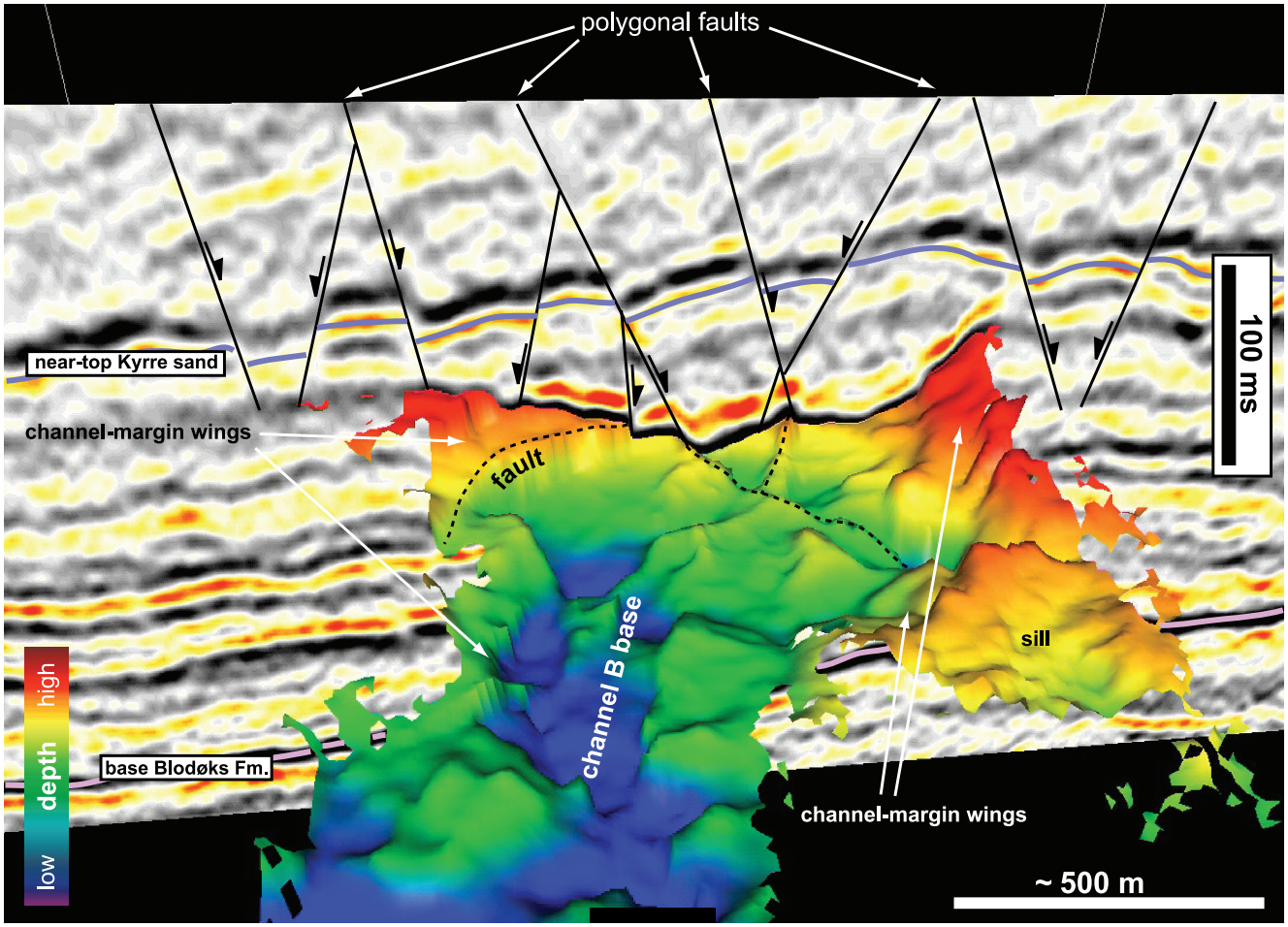

FIGURE 10. Perspective view of submarine channel B illustrating the straight geometry of the channel and the development of laterally continuous wings at the channel margins. A polygonal fault network is developed in the mud-dominated stratigraphy, encasing the channel, and is clearly seen to offset both the near-top Kyrre sand seismic horizon the wing structure that developed along the northern flank of the channel and the channel itself. Location of viewpoint is indicated in Figure 5a.

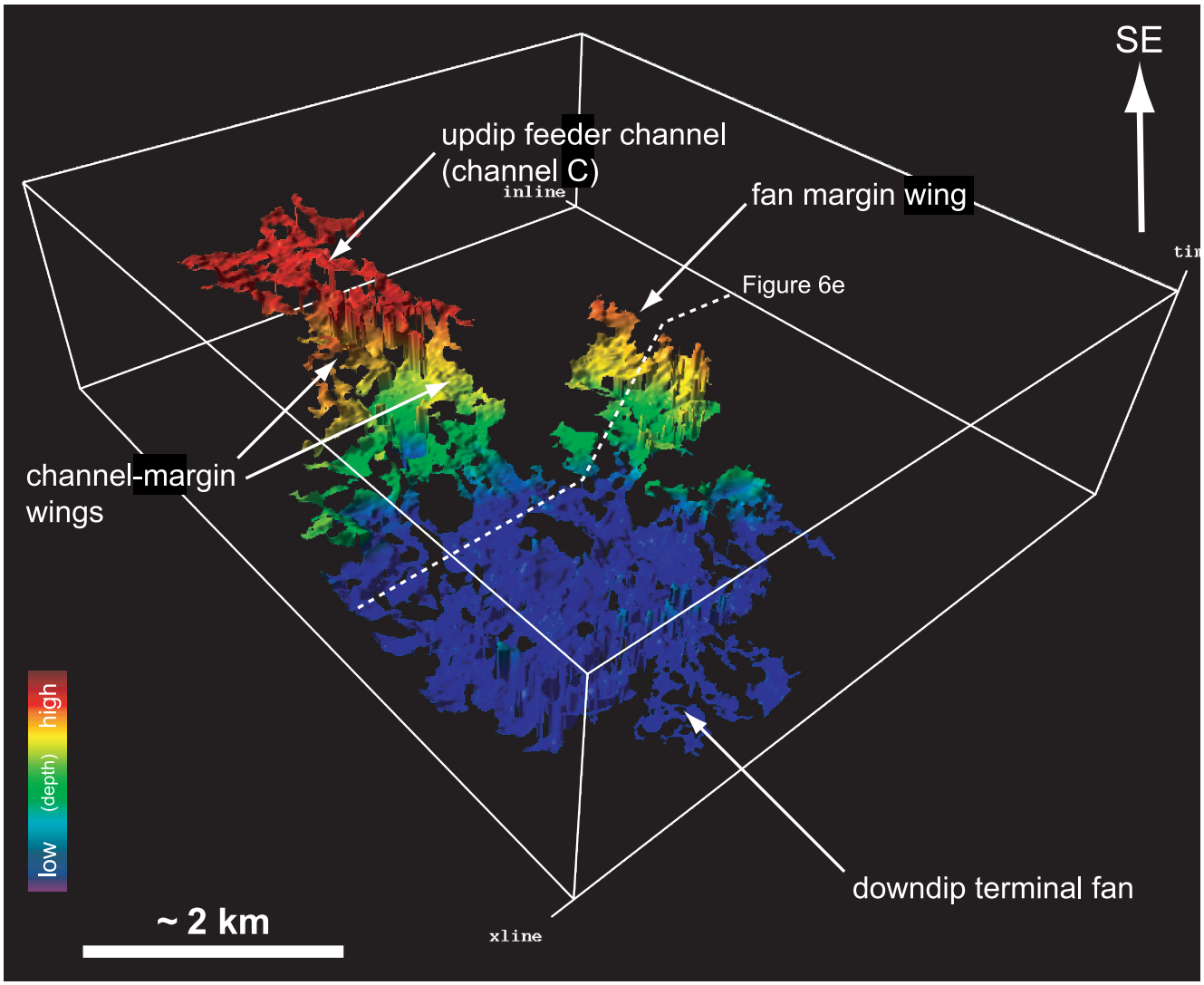

FIGURE 11. Perspective view of the interpreted channel C and the terminal fan developed at its downdip end. Laterally continuous wings are observed along the margins of the channel, whereas the wing feature associated with the terminal fan only occurs along an about 1-km portion of its the southern margin (see Figure 6e). Location of viewpoint is indicated in Figure 5a. The location of Figure 6e is marked.

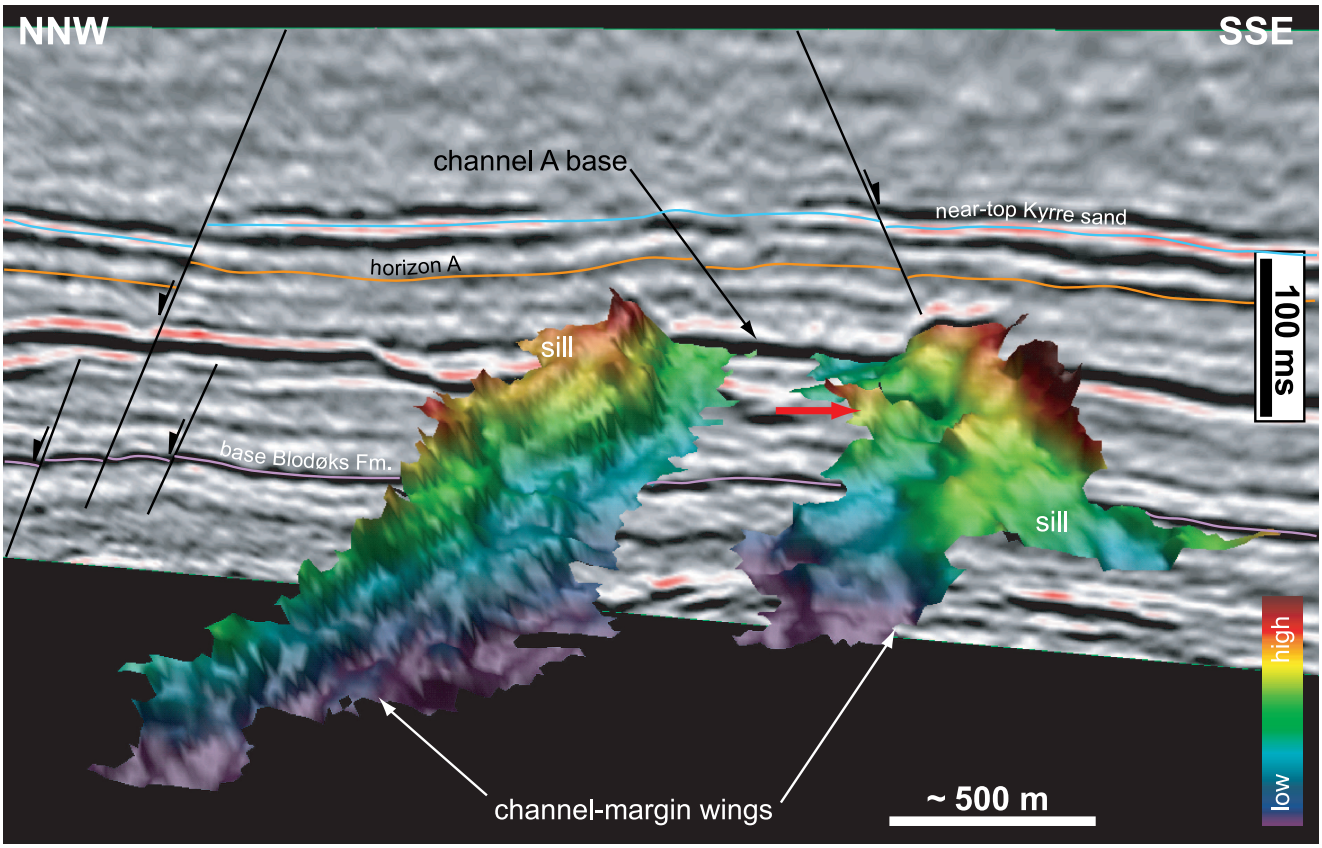

FIGURE 12. Perspective view illustrating the geometry of laterally continuous wing structures flanking submarine channel A. Along the southern wing structure, a smaller, subordinate wing structure branching off the main channel-margin wing is observed (arrowed red). These features are interpreted as clastic dikes formed by the remobilization and injection of clastic material from the primary depositional channel sand body. See Figure 5a for the location of viewpoint.

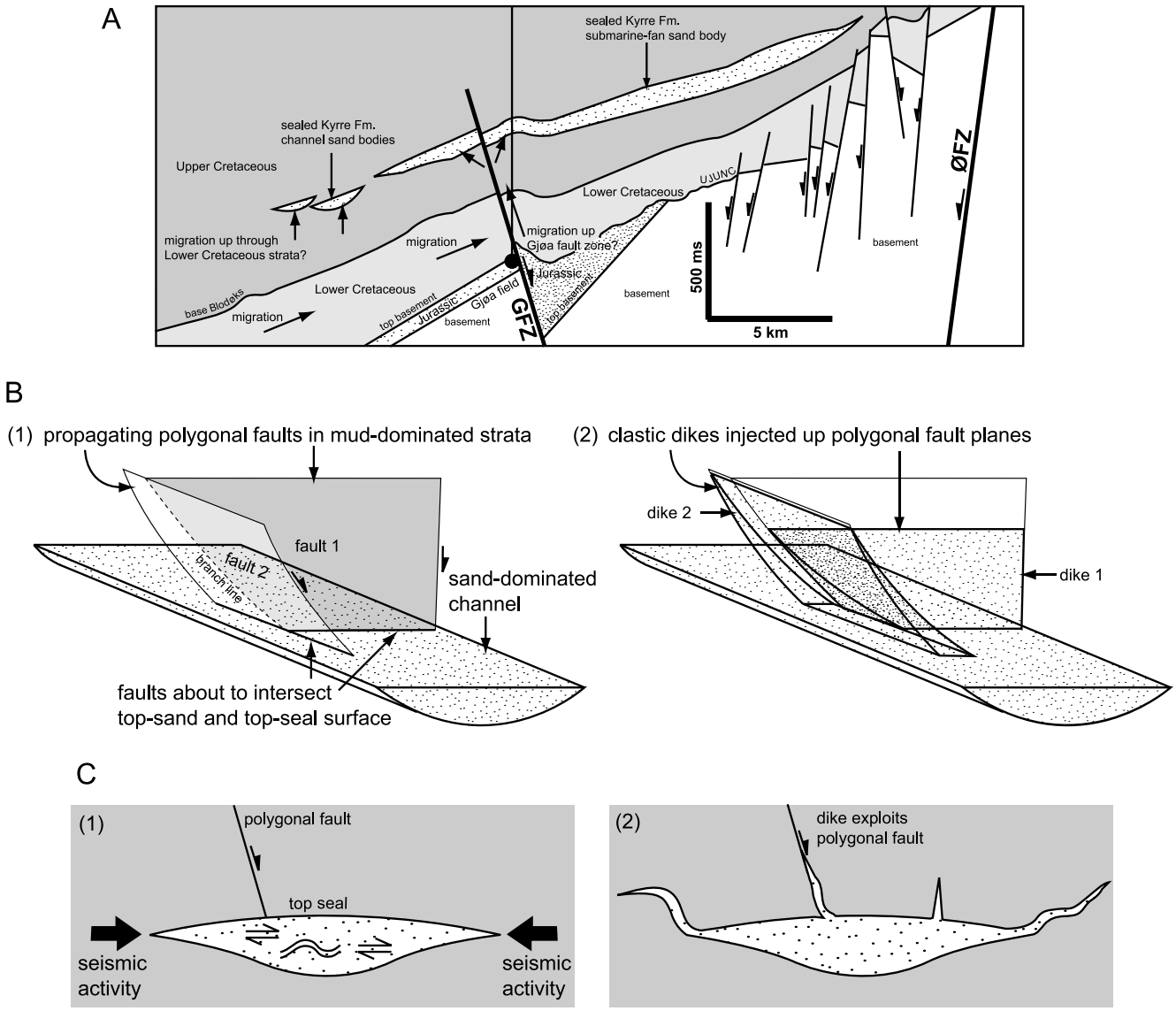

FIGURE 13. Conceptual diagrams illustrating the potential triggering mechanisms for remobilization and injection of the sand in the Kyrre Formation channels. (a) Overpressure development and top-seal failure caused by flow of basinal fluids (hydrocarbon and/or water) into a sealed sand body. (b) Top-seal failure and sand fluidization in response to propagating polygonal faults. (c) Top-seal failure and fluidization caused by shear associated with seismic shaking. ØFZ = Øygården fault zone; GFZ = Gjøa fault zone; UJUNC = Upper Jurassic unconformity.

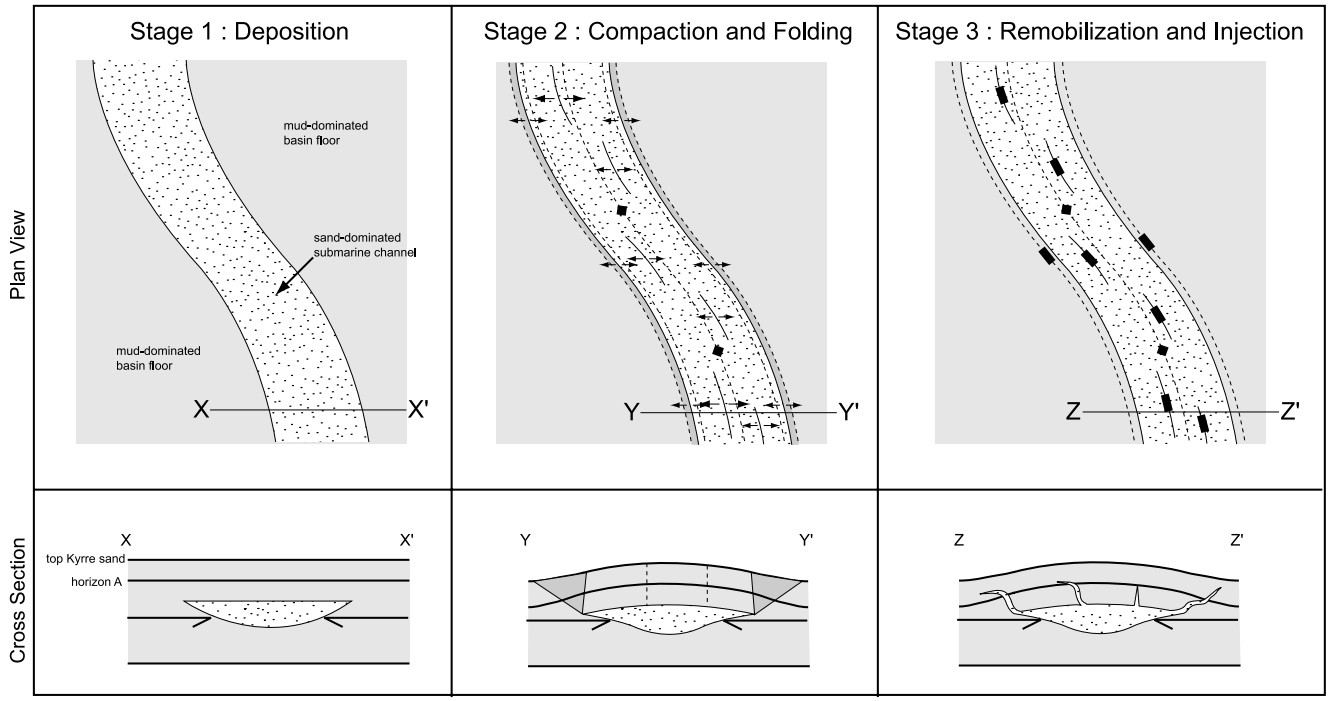

FIGURE 14. Conceptual diagrams illustrating the development of clastic injections adjacent to one of the Kyrre Formation channels in response to differential compaction and associated forced folding. Stage 1 = sands are deposited in an erosively based submarine-channel complex in a mud-dominated slope to basin-floor setting. The channel is gradually buried in muds. Stage 2 = differential compaction causing partial inversion and mounding of the channel. Extensional stresses develop at the margin and locally along the crest of the channel because of folding of the strata over the channel. Stage 3 = laterally persistent fractures and/or low-displacement faults develop at the zones of extensional strain at the channel margins, whereas more locally developed fractures and/or faults develop along the axis of the channel. Injections above the main parent sand body are focused along these planes of weakness resulting in (1) their preferential development at the margins of the channels, (2) their elongate alignment along the channel margins, and (3) their channel parallel orientation where they developed above the axes of the channels.